REPUBLIQUE ALGERIENNE DEMOCRATIQUE ET POPULAIRE
MINISTERE DE L'ENSEIGNEMENT SUPERIEUR ET DE LA RECHERCHE SCIENTIFIQUE
UNIVERSITE MOHAMED BOUDIAF - M'SILA

FACULTE : SCIENCES **DOMAINE : SCIENCE DE LA MATIERE**
DEPARTEMENT : PHYSIQUE **FILIERE : PHYSIQUE**
N° :…….. **OPTION : PHYSIQUE APPLIQUÉE**

Mémoire présenté pour l'obtention
Du diplôme de Master Académique

Par: ABDELLAHOUM LEÏLA

Intitulé

Calculation of structural, electronic, elastic and optical properties of 2H-CuGaO2: First principle study.

Soutenu le 27/05/2017 devant le jury composé de:

Pr. SAIB Salima	Universite Mohamed Boudiaf - M'sila	Président
Pr. DEGHFEL Bahri	Universite Mohamed Boudiaf - M'sila	Rapporteur
Pr. IBRIR Miloud	Universite Mohamed Boudiaf - M'sila	Examinateur

Année universitaire : 2016/2017

Acknowledgements

*First and foremost, El hamdou Li « **Allah** » who has given me his beneficent so that I am able to finish this work , peace and Salam are always blessed and powered down upon our beloved prophet Muhammad SAW as the last messenger that has shown us the right way.*

*I would like to thank very much my academic supervisor, Prof. **DEGHFEL Bahri.** His helpful door was always open whenever I ran into a trouble spot or had a question about my research or writing He consistently allowed this dissertation to be my own work, but steered me in the right direction whenever he thought I needed it. I am grateful for his special advises for me and especially supporting my desire to writing this work in English. I hope Allah bless him and his family .*

*I would also like to thank the jury members Prof. Madame SAIB Salima and Prof. IBRIR Miloud, from university of **MOHAMED Boudiaf** of M'sila, for accepting evaluate this work.*

I would also like to acknowledge all my teachers of department of physics.

I am also thankful to all those who have always prayed for me and besought God to help me.

Abdellahoum leïla

DEDICATION

*Above all I would like to thank the almighty **ALLAH**, the lord of the universe, my creator, my strong pillar, my source of inspiration, wisdom, knowledge and understanding. For all the strength and perseverance he has installed in me during all the years of my studies, without him this work wouldn't have been started. We will always be in the shelter of **ALLAH** from now and until hereafter life. Amine.*

*I dedicate my humble efforts for my "heaven on earth" , my parents ; a strong and gentle souls who taught me to trust in **ALLAH** , supporting and encouraging me to believe in hard work*

For their prayers

For their sacrifices

And for their endless patience.

﴿....And say my lord be merciful to them as they brought me up when I was little ﴾Al-Isra v.N:24

For my six brothers and three sisters and all their children and for my fiance and his family.; all have given me a loving environment where to develop. How grateful I'm with you. Thank you, you have always supported and encouraged me to do my best in all matters of life.

*I cannot finish without mention with who I have shared experiences in life my best friend **MECHTER IMANE** the one who brings out the best on me she were always been there for me to lend hand in good time and bad I really treasure our friendship, and for my friends I care and love **B.MALIKA S.HIBA B.SOULTANA REBIKA M.DOUNIA B.ZOHRA.***

*I am also thankful to my field study fellows (particularly **SARA SAADEDDIN** ,and all the friends **Halima ZANAT , IMAN BARKAT LADMIA.L , FATIMA.R, saadia.A, AMAL.B,WAFA.A**,) for all the best time we shared together.*

And for all who know

ABDELLAHOUM LEILA

Contents

CHAPTER 3: Results & discussion

GENERAL INTRODUCTION

Introduction

CuGaO2 belongs to the delafossite structure with the general formula AMO_2 and has been studied due to its intrinsic p-type conductivity. As we know, solids with wide band gap usually exhibit insulating behavior but some of the metal oxides with wide gap are made to conduct. Such transition metal oxides are called transparent conducting oxides (TCO). Transparent conducting oxide materials are noble metal oxides of the form AMO_2 (A = Cu, Pd and M = Al, In, Fe, Ga, etc.) that crystallize in the simple delafossite structure [1]. The majority of transparent conduction oxides (TCOs) are n-type conductors such as ZnO,SnO2 and In2O3 [2-3]. It is until 1997 that p-type conductivity of CuAlO2 has been firstly found by Kawazoe et al. [4] and has received great attentions [3–7]. CuGaO2, with the same delafossite structure, is an important p-type transparent conducting oxide for both fundamental science and industrial applications [5],whereas such materials could open the way to a range of novel applications. For example, a combination of the two types of transparent conductor in the form of a p-n junction could lead to a 'functional' window that transmits visible light yet generates electricity in response to the absorption of ultraviolet photons [4] and it can be used also in the p-channel transparent transistor, oxygen storage capacity, photo catalysts, thermoelectric energy conversion devices, UV emitting diodes, solar cells, optical displays, low emissivity and electro chromic windows, etc. [6-7].

It can be seen that many works have taken account of structural and electronic properties, but the elastic and optical and optoelectronic properties that are basic physical properties and important to technological and industrial applications delafossite semiconductors have seldom been reported to date,

The most common CuGaO2 structures are trigonal 3R ($R\bar{3}m$, D53d) and hexagonal 2H (P63/mmc,D46h) [1-9]. The difference between these two structures is the stacking of successive layers of MO_6 octahedra. Thus, systemic studies on 3R-and 2H-CuGaO2 of basic physical properties are of great importance and in demand. More recently, efforts have been devoted to develop CuGaO2 both experimentally [6-7] and theoretically [1, 9–13]. Nie et al.

[14] have studied the electronic and optical properties of 3R-CuGaO2 to investigate bipolar doping and band-gap anomaly using local density approximation (LDA) and general potential linearized augmented plane wave (LAPW) method with WIEN97 code. The structural and electronic properties of 3R- and 2H-CuGaO2 have been calculated using self-consistent tight binding linear Muffin- Tin orbital(TB-LMTO) method [1], periodic Hartree–Fock method and posteriori density-functional corrections [9], pseudo potential method with B3LYP functional [10] and LMTO calculations with the Stuttgart TB-LMTO-ASA code [12].

CuGaO2 follows the same rules in the delafossite families and has received considerable interests recently due to its energy gap for direct allowed transition was estimated to be 3.6 eV and its anodic applications [15]. To our knowledge, the reports based on the photoluminescence properties of $CuGaO_2$ have not been published so far, and the application researches which have been reported were concentrated on transparent conductive film or p-type dye-sensitized solar cells [16]. The present work, which is devoted to present first-principles calculations of structural, elastic ,mechanical, electronic and optical properties of 2H-CuGaO2 compound, is organized as follows:

In the first chapter, we describe the fundamental mathematical problem needed to solve the many-body quantum mechanics for a system of nuclei and electrons where the Born-Oppenheimer approximation are used to simplify it by separating the nuclear and electronic degrees of freedom and outline the different methods to remedy, either approximately or exactly, this problem. The Density functional theory (DFT), exact method, as developed by Kohn-Sham is outlined in this work. It requires the approximation of exchange and correlation functional of the electronic density for practical use. At the end of this chapter we needed to define an appropriate basis set to expand the Kohn-Sham wave functions and express the different parts of the Hamiltonian for periodic systems to solve the Kohn-Sham equations in order to get the ground state energy.

In the second chapter, a preview is given about the CASTEP code used in the present work in order to simulate the physical properties of the considered system.

The last chapter, is devoted to present and discuss the obtained results of 2H-CuGaO2 compound.

Finally, a brief conclusion is given about the obtained results.

Bibliography:

[1] V. Jayalakshmi, R. Murugan, B. Palanivel, Journal of Alloys and Comp. 388 (2005) 19.

[2] U. Ozgur, Ya.I. Alivov, C. Liu, A. Teke, M.A. Reshchikov, S. Dogan, V. Avrutin, S.-J. Cho, H. Morkoc, J. Appl. Phys. 98 (2005) 041301.

[3] J. Bandara, C.M. Divarathne, S.D. Nanayakkara, Sol. Energy Mater. Sol. Cells 81(2004) 429.

[4] H. Kawazoe, M. Yasukawa, H. Hyodo, M. Kurita, H. Yanagi, H. Hosono, Nature (London) 389 (1997) 939.

[5] M. Yu, I Thomas. Draskovic, and Y. Wu, Inorg. Chem. *53* (2014) 5845.
[6] T. Mine, H. Yanagi, K. Nomura, T. Kamiya, M. Hirano, H. Hosono, Thin Solid Films 516 (2008) 5790. 3

[7] S. Kato, R. Fujimaki, M. Ogasawara, T. Wakabayashi, Y. Nakahara, S. Nakata, Appl. Catal. B: Environ. 89 (2009) 183.

[8] K. Gurunathan, J.-O. Baeg, S.M. Lee, E. Subramanian, S.-J. Moon, K.-Jeong Kong, Catal. Commun. 9 (2008) 395.

[9] A. Buljan, P. Alemany, E. Ruiz, J. Phys. Chem. B 103 (1999) 8060.
[10] J. Robertson, P.W. Peacock, M.D. Towler, R. Needs, Thin Solid Films 411 (2002) 96.
[11] J. Pellicer-Porres, A. Segura, Ch. Ferrer-Roca, D. Martı´nez-Garcı´a, J.A. Sans, E. Martı´nez, J.P. Itie ´, A. Polian, F. Baudelet, A. Mun ˜oz, P. Rodrı´guez-Herna ´ndez, P. Munsch, Phys. Rev. B 69 (2004) 024109.

[12] H.C. Kandpal, R. Seshadri, Solid State Sci. 4 (2002) 1045.

[13] Z.-J. Fang, C. Fang, L.-J. Shi, Y.-H. Liu, M.-C. He, Chin. Phys. Lett. 25 (2008) 2997.

[14] X. Nie, S.-H. Wei, S.B. Zhang, Phys. Rev. Lett. 88 (2002) 066405.

[15] K. Ueda, T. Hase, H. Yanagi, H. Kawazoe, H. Hosono, H. Ohta, M. Orita, M. Hirano. J. Appl. Phys. 89 (2001)1790–1793.

[16] L. Shi, F. Wang, Y. Wang, D. Wang, B. Zhao, L. Zhang, D. Zhao & D. Shen, Scientific reports 6 (2016) 21135.

CHAPTER I:

Theoretical background:

Density Functional Theory (DFT)

CHAPTER I:

Theoretical Background :

Density Functional Theory (DFT)

I. 1 Introduction

The ground-state theory in which the emphasis is on the charge density as the relevant physical quantity is Density Functional Theory (DFT), which has proved to be highly successful in describing structural and electronic properties in a vast class of materials, ranging from atoms and molecules to simple crystals to complex extended systems.

The science of materials and condensed matter are fundamentally concerned with the understanding and the exploitation of their physical properties. This is well known since the development of quantum mechanics that is very successful in describing the physical properties of very small systems, which the Newtonian mechanics fails to describe [1].

The equations developed within the theory of quantum mechanics are quite complicated to be solved analytically. Fortunately, it is practically possible for scientists to treat bigger system due to continuous development of various computational methods and solve the equations numerically [1].

I. 2 Schrödinger Equation :

In 1962, the physicist Autrichien Schrödinger [2] proposed a basic theoretical equation for non-relativistic quantum in time-independent system which describes all the interactions between the nucleus and the electrons within a crystalline body. The basic equation to be solved is the Schrödinger equation, does not give the trajectory of a particle, but rather the

wave function of the quantum system, which carries information about the wave nature of the particle. It can be written as :

$$\hat{H}(\{\mathbf{R}_I\},\{\mathbf{r}_i\}) = E\Psi(\{\mathbf{R}_I\},\{\mathbf{r}_i\}) \quad \textbf{(I.1)}$$

With $\Psi(\{\mathbf{R_I}\},\{\mathbf{r_i}\})$ is the wave function, E is the total energy of the system, $\hat{H}$ is the Hamiltonian describing this interaction, which can be written as:

$$H = -\frac{\hbar^2}{2m}\sum_i^n \nabla_i^2 - \frac{\hbar^2}{2}\sum_k^N \frac{\nabla_k^2}{M_k} + \frac{1}{2}\sum_i^n \sum_{i\neq j}^n \frac{e^2}{4\pi\varepsilon_0 r_{ij}} + \frac{1}{2}\sum_k^N \sum_l^N \frac{Z_k Z_l e^2}{4\pi\varepsilon_0 R_{kl}} + \sum_i^n \sum_k^N \frac{Z_k e^2}{4\pi\varepsilon_0 r_{ik}} \quad \textbf{(I .2)}$$

Where the nucleus (electron) has the position R_k (r_k), the mass M_k (m_k) and the charge Z_k (e) and R_{kl} (r_{ik}) is the distance between nuclei (electrons).

The Hamiltonian ***H*** can be written in another way as :

$$H = T_e + V_{ee} + V_{eN} + T_N + V_{NN} \quad \textbf{(I.3)}$$

Where

$\mathbf{T_e}$ **:** is the kinetic energy of the electrons,

T_N : is the kinetic energy of the nucleus,

V_{ee} : is the potential energy of repulsion electron-electron,

V_{NN} : is the potential energy of repulsion nuclei-nucleus,

V_{eN} : is the potential energy of attraction electron-nucleus.

The Schrodinger equation **(I.1)** contains (3N+3n+n degrees of freedom), which means that its resolution is very complicated task. This implies the use of some approximations.

I.3 Born-Oppenheimer Approximation:

In 1927, the physicists Born and Oppenheimer [3] published a theoretical simplified method to calculate molecule wave function and they recognized that the atomic nuclei are more massive particles than the electrons and, as a result, their velocities are much lower.

The nuclei can be considered as stationary with electrons following the motion of the nuclei[1]. Therefore, their behavior practically dose not modified by the low displacement, so we can eliminate the term T_N (considering V_{NN} = constant). This allows to rewrite a new equation for the electronic wave function given by :

$$\mathbf{H = T_e + V_{ee} + V_{eN}} \qquad \textbf{(I.4)}$$

So :

$$\boldsymbol{H_e} = -\frac{\hbar^2}{2m}\sum_i^n \boldsymbol{\nabla_i^2} + \frac{1}{2}\sum_i^n \sum_{i\neq j}^n \frac{e^2}{4\pi\varepsilon_0 r_{ij}} - \sum_i^n \sum_k^N \frac{Z_k e^2}{4\pi\varepsilon_0 r_{ik}} \qquad \textbf{(I.5)}$$

Within the framework of this approximation, the wave function in Schrödinger equation becomes depending only on electrons ones $\boldsymbol{\Psi_{electron}}$ [1]:

$$\hat{H}_{electron}\, \boldsymbol{\Psi}_{electron} = \mathbf{E}_{electron}\, \boldsymbol{\Psi}_{electron} \qquad \textbf{(I.6)}$$

A large number of electrons interaction between themselves makes difficult the resolution of the equation **(I.3) [4].**

I . 4 Hartree and Hartree-Fock Approximation:

The first approach solution to the equation (I.3) was in 1928 by Hartree. This approximation reduced the problem of the interaction of N electrons to a unique electron system [4].

So, the Hamiltonian could be written as a sum of Hamiltonians, each one write the behavior of one electron :

$$\boldsymbol{H} = \sum_i \boldsymbol{H_i} \qquad \textbf{(I.7)}$$

With

$$H_i = -\frac{\hbar^2}{2m}\Delta_i + U_i(\boldsymbol{r_i}) + V_i(\boldsymbol{r_i}) \qquad \textbf{(I .8)}$$

Such as :

$$U_i(\boldsymbol{r_i}) = -\sum_k \frac{Z_k e^2}{4\pi\varepsilon_0 |r_i - R_k^0|} \qquad \textbf{(I.9)}$$

$\boldsymbol{U_i(r_i)}$: Potential energy of the electron (i) in the field of all nuclei [$V_N(\boldsymbol{r_i})$.]

Also, the effective field of Hartree is given by :

$$V_i(\boldsymbol{r}_i) = \frac{1}{2}\sum_j \frac{e^2}{4\pi\varepsilon_0|\boldsymbol{r_i}-\boldsymbol{r_j}|} \quad \textbf{(I.10)}$$

Then, the effective potential is the sum of the two contributions :

$$V_{eff}(\boldsymbol{r}) = V_H(\boldsymbol{r}) + V_N(\boldsymbol{r}) \quad \textbf{(I.11)}$$

Introducing the effective potential in the Schrödinger equation, we found ;

$$-\frac{\hbar^2}{2m}\nabla^2\Psi_i(\boldsymbol{r}) + V_{eff}(\boldsymbol{r})\Psi_i(\boldsymbol{r}) = E_i\Psi_i(\boldsymbol{r}) \quad \textbf{(I.12)}$$

The electronic system wave function has a form of a product of waves functions of electrons, and the sum of all electrons energy is equal to the system energy :

$$\Psi(\vec{\mathrm{r}}_1, \vec{\mathrm{r}}_2, \ldots\ldots\ldots, \vec{\mathrm{r}}_\mathrm{n}) = \Psi_1(\vec{\mathrm{r}}_1)\Psi_2(\vec{\mathrm{r}}_2)\ldots\ldots\ldots\Psi_\mathrm{n}(\vec{\mathrm{r}}_\mathrm{n}) \quad \textbf{(I .13)}$$

$$E=E_1+E_2+\ldots\ldots\ldots+E_n \quad \textbf{(I.14)}$$

In 1930, Fock showed that Hartree's wave function violates Paul's exclusion principle because it isn't antisymmetric with respect to the exchange of any two particles. To correct this default Hartree, Fock and Slater have shown that the Hartree antisymmetric wave function is written in the form of a Slater determinant and satisfies the Pauli principle:

$$\Psi(\vec{\mathrm{r}}_1, \vec{\mathrm{r}}_2, \ldots\ldots\ldots, \vec{\mathrm{r}}_\mathrm{n}) = \frac{1}{\sqrt{\mathrm{N!}}}\begin{vmatrix} \Psi_1(\vec{\mathrm{r}}_1) & \Psi_1(\vec{\mathrm{r}}_2) & \ldots & \Psi_1(\vec{\mathrm{r}}_\mathrm{n}) \\ \Psi_2(\vec{\mathrm{r}}_1) & \Psi_2(\vec{\mathrm{r}}_2) & \ldots & \Psi_2(\vec{\mathrm{r}}_\mathrm{n}) \\ \vdots & \vdots & & \vdots \\ \Psi_\mathrm{n}(\vec{\mathrm{r}}_1) & \ldots & & \Psi_\mathrm{n}(\vec{\mathrm{r}}_\mathrm{n}) \end{vmatrix} \quad \textbf{(I.15)}$$

I. 5 The density functional theory :

DFT is an extremely successful approach for the description of ground state properties of an electronic system such as: metals, semiconductors and insulators. It is extensively used to study bulk materials and it also treats successfully the complex materials such as carbohydrates, proteins or carbon nanotubes [5].

The fundamental concept of the density functional is that the energy of a system can be expressed as a function of the electron density ρ0**(r)** which minimizes the energy of the system. The use of electronic density as a fundamental variable to describe the properties of the system has been existing since the earliest approaches to the electronic structure of matter but It has obtained proof only by the demonstration of the two fundamental theorems of Hohenberg and Kohn (1964) as well as of Kohn and Sham (1965) who presented the best procedure for realizing the DFT [4].

I. 5. 1 what is the electronic density? :

The electronic density is a measure of the probability of an electron occupying an infinitesimal element of space $\boldsymbol{dr^3}$ surrounding any given point. It is given as;

$$\boldsymbol{\rho(r)} = \int \boldsymbol{dr_2} \dots \int \boldsymbol{dr_n}\, \boldsymbol{\Psi^*(r, r_2, \dots r_n)\Psi(r, r_2, \dots r_n)} \qquad \textbf{(I.16)}$$

I. 5. 2 The Thomas –Fermi Model:

The base of Thomas (1926) and Fermi (1928) model is to describe the system energy as a simple function of density [5], which is the main origin of the DFT actually. Therefore , the total energy of Thomas-Fermi, using the kinetic energy expression and considering the electron-nuclei and electron-electron contribution, is given by ;

$$E = \boldsymbol{T_{TF}} + \int V(\boldsymbol{r})\,\rho(\boldsymbol{r})d\boldsymbol{r} + \frac{1}{2}\int \frac{\rho(\boldsymbol{r})\rho(r')}{|\boldsymbol{r}-\boldsymbol{r}'|} d\boldsymbol{r}d\boldsymbol{r}' \qquad \textbf{(I.17)}$$

=Kinetic Energy + External Potential (due to nuclei) + Electron- Electron Interaction

$\boldsymbol{T_{TF}}$ **:** is the kinetic energy given as**:**

$$\boldsymbol{T_{TF} = C_F \int \rho(r)^{5/3} dr} \quad \textbf{(I.18)}$$

with C_F= 3(3π^2)$^{2/3}$/10].

This model fails to explain the exchange and correlation effects and does not give a binding energy for molecules. Therefore, Dirac in 1930 [4], proposed a correction that represented the exchange effects into the de Thomas-Fermi function $E_X(\rho)$.

So, the total energy of Thomas-Fermi expression can take another form:

$$E_{TF} = C_F \int \rho^{\frac{5}{3}}(r) d\boldsymbol{r} + \int V(r)\, \rho(r) d\boldsymbol{r} + \frac{1}{2} \int \frac{\rho(\boldsymbol{r})\rho(r')}{|\boldsymbol{r}-\boldsymbol{r}'|} d\boldsymbol{r} d\boldsymbol{r}' - C_X \int \rho^{\frac{4}{3}}(r) d\boldsymbol{r} + \int \rho^{\frac{4}{3}}(r) d\boldsymbol{r} / (C_C' + \rho^{\frac{1}{3}}(r)) \quad \textbf{(I.19)}$$

With :

$\boldsymbol{C_X}$= 3(3/π)$^{1/3}$ /4, C_c=- 0.056 and C_C'=- 0.079.

I. 5.3. Hohenberg-Kohn Theorems :

The foundation of DFT has been started to be developed by the two fundamental theorems of Hohenberg and Kohn [6]:

Theo.1: for an external potential V_{ext}(r), the total energy of the ground state is uniquely functional of the particles density **ρ(r).** Hence the total energy functional of the ground state, is given by :

$$E_0 = T[\rho_0] + E_{ne}[\rho_0] + E_{ee}[\rho_0] \quad \textbf{(1.20)}$$

Theo.2: Hohenberg et Kohn showed that the real ground-state density **ρ**(r) is the one that minimizes the total energy functional **E[ρ]** of all the system with many-body particles

according to the variational principle for an electronic charge density functional $\boldsymbol{\delta E/\delta \rho|_{\rho_0} = 0}$. So, the ground-state particles density satisfies [4]:

$$E_0 = \min_\rho E[\rho(r)] \qquad \textbf{(1.21)}$$

In principle, by varying ρ(r), E_0 can be found to minimize **E[ρ(r)].**

Also, the energy functional can be written in terms of the external potential and another functional $\boldsymbol{F_{HK}[\rho]}$:

$$\boldsymbol{E[\rho(r)] = F_{HK}[\rho(r)] + \int V_{ext}[\rho(r)]\, dr} \qquad \textbf{(I.22)}$$

$\boldsymbol{F_{HK}[\rho]}$ includes the kinetic energy and electron-electron terms[5] as :

$$F_{HK}[\rho(r)] = T[\rho(r)] + E_{ee}[\rho(r)] \qquad (\mathbf{I.23})$$

But the theorems give no information about how to construct the functional. Kohn and Sham then proposed a simple method where they replace many-body problem with an independent electron one that can be solved.

I. 5.4. Kohn-Sham formalism :

In 1965, Kohn and Sham, introduced a fictitious system that replace the interacting system with an equivalent system of non- interaction electrons moving in an effective potential chosen such that its ground state electron density is the same as the one of the true system.[1]

The Hamiltonian for this system can be written as:

$$\boldsymbol{\hat{H}_{KS}(r) = -\frac{1}{2}\sum_{i=1}^{n} \nabla_i^2 + \sum_{i=1}^{n} V_{eff}(r_i)} \qquad (\mathbf{I.24})$$

Where $\hat{H}_{KS}$ is the Kohn-Sham mono-electronic Hamiltonien operator.

According to Hohenberg-Kohn theory, the energy of this system is described as**[5]:**

$$E[\rho(r)] = T_s[\rho(r)] + \int V_{ext}[\rho(r)]\, dr \qquad \textbf{(I.25)}$$

With $\boldsymbol{T_s[\rho(r)]}$ is the kinetic energy of the non-interacting system.

The charge density can be written as:

$$\rho(\boldsymbol{r}) = \sum_{occup} |\varphi_i(\boldsymbol{r})|^2 \qquad \textbf{(I.26)}$$

Then, the universality of total energy functional of Kohn-Sham, $F_{\mathrm{KS}}[\rho]$, is written as :

$$F_{KS} = T_S[\rho] + \tfrac{1}{2}\iint \frac{\rho(\boldsymbol{r})\rho(\boldsymbol{r}')}{|\boldsymbol{r}-\boldsymbol{r}'|} d\boldsymbol{r}d\boldsymbol{r}' + E_{XC}[\rho] \qquad \textbf{(1.27)}$$

Where:

$\boldsymbol{\frac{1}{2}\iint drdr'\frac{\rho(r)\rho(r')}{|r-r'|}}$ **;** is the classical electrostatic energy of Hartree E_{H}.

$\boldsymbol{E_{XC}[\rho]}$ **:is** the exchange-correlation energy.

So, the energy functional for the real system can be described to include the kinetic energy $\boldsymbol{T_s}$ of the non-interacting system as :

$$E_{KS}[\rho] = T_S[\rho] + \tfrac{1}{2}\iint d\boldsymbol{r}d\boldsymbol{r}'\frac{\rho(\boldsymbol{r})\rho(\boldsymbol{r}')}{|\boldsymbol{r}-\boldsymbol{r}'|} + E_{XC}[\rho] + \int V_{ext}(\boldsymbol{r})\rho(\boldsymbol{r})d\boldsymbol{r} \qquad \textbf{(I.28)}$$

We have to minimizing E_{KS} for the effective potential V_{eff} by applying the variational principle.

The functional energy correspondent to the Hamiltonian $\hat{H}_{\mathrm{KS}}$ (I.22) is :

$$E_{V_{eff}}[\rho'] = T_S[\rho'] + \int V_{eff}(\boldsymbol{r})\rho'(\boldsymbol{r})d\boldsymbol{r} \qquad \textbf{(I.29)}$$

So :

$$V_{eff}(\boldsymbol{r}) = V_{ext}(\boldsymbol{r}) + \underbrace{\iint \frac{\rho(r')}{|\boldsymbol{r}-\boldsymbol{r}'|}dr'}_{V_H} + \underbrace{\frac{\delta E_{XC}[\rho]}{\delta\rho}}_{V_{XC}} \qquad \textbf{(I.30)}$$

It then follows that by solving the Schrödinger equation for no interacting particles moving under the influence of an effective potential :

$$\left\{-\frac{\hbar^2}{2m}\nabla^2 + V_{eff}\right\}\Psi_i(r) = C_i\ \Psi_i(r) \qquad \textbf{(I.31)}$$

I. 5.5. Exchange-Correlation Functional :

I. 5.5.1. Local Density Approximation (LDA):

The simplest approximation is to assume that the density can be treated locally as an uniform electron gas; the exchange correlation energy at each point in the system is the same as that of an uniform electron gas of the same density. This approximation was originally introduced by Kohn and Sham [7] and holds for a slowly varying density. Using this approximation the exchange-correlation energy for a density $\boldsymbol{\rho(r)}$ is given by ;

$$E_{XC}^{LDA}[\rho(r)] = \int \varepsilon_{XC}^{LDA}[\rho(r)]\rho(r)dr \qquad \textbf{(I.32)}$$

$\varepsilon_{XC}^{LDA}[\rho(r)]$: is the exchange-correlation energy density per particle of an uniform electron gas of density ρ(r).

The exchange-correlation potential is then given by:

$$v_{XC}^{LDA}[\rho(r)] = \frac{\delta E_{XC}^{LDA}}{\delta\rho(r)} = \varepsilon_{XC}^{LDA}[\rho(r)] + \rho(r)\frac{\delta E_{XC}^{LDA}}{\delta\rho(r)} \qquad \textbf{(I.33)}$$

The LDA is usually parameterized by separating the energy $E_{XC}^{LDA}[\rho(r)]$ into the exchange energy and correlation energy for the homogenous electron gas of density $\rho(r)$:

$$E_{XC}^{LDA}[\rho(r)] = E_X^{LDA}[\rho(r)] + E_C^{LDA}[\rho(r)] \qquad \textbf{(I.34)}$$

The exchange energy is a simple analytical form and comes from the Dirac's exchange formula (Dirac, 1930)[5]:

$$\mathbf{E_X^{LDA}[\rho(r)] = -C_X \int \rho^{\frac{4}{3}}(r)dr} \quad \textbf{(I.35)}$$

Where :$-C_X = -3/4\sqrt[3]{3/\pi}$.

This method is often a very effective approximation. It is found to work reasonably well in semiconductors and insulators, because it is considered to provide suitable results for slowly varying density systems and It also works better in the systems where the charge density is rapidly varying. However, LDA has some disadvantages such as the systematic underestimation of the solid cohesion energy [5].

I. 5.5.2.Generalized Gradient Approximation (GGA):

In the Generalized Gradient Approximation (GGA) method. The exchange-correlation energy becomes a functional of the charge density and its gradient. Symbolically it can be written as :

$$E_{xc}^{GGA}[\rho] = \int \rho(\boldsymbol{r}) f[\rho(\boldsymbol{r}).\nabla\rho(\boldsymbol{r})]d\boldsymbol{r} \quad \textbf{(I.36)}$$

Also, the exchange and correlation GGA are treated separately as:

$$E_{xc}^{GGA}[\rho(\boldsymbol{r}).\nabla\rho(\boldsymbol{r})] = E_x^{GGA}[\rho(\boldsymbol{r}).\nabla\rho(\boldsymbol{r})] + E_c^{GGA}[\rho(\boldsymbol{r}).\nabla\rho(\boldsymbol{r})] \quad \textbf{(I.37)}$$

Where $\nabla\rho(\boldsymbol{r})$ is the electronic gradient of charge density.

There are several works shown that the GGA approximation did important improvements than does the LDA approximation, such as the PW91 and PBE functionals (Perdew et al., 1996, Perdew and Yue, 1986) [5], which are applied to several systems (iron for example).

I. 6.Bloch's Theorem and Plane Wave Basis Sets :

In 1929, Felix Bloch [1], discussed the main difficulties to overcome: a wave function has to be calculated for each of the infinite number of electrons which will extend over the entire space of the solid and the basis set in which the wave function will be

expressed will be infinite. The ions in a perfect crystal are arranged in a regular periodic way. Therefore, the external potential felt by the electrons will also be periodic. That is on an electron at position $\boldsymbol{r}$ can be expressed as $V_{ext}(\boldsymbol{r})=V(\boldsymbol{r}+\boldsymbol{R})$. This request needed for the use of Bloch's theorem, which makes it possible to express the electronic wave functions at each k-point can be expanded in terms of discrete plane-wave basis sets (infinite Fourier series) which are popular in calculations involving periodic boundary conditions for three dimensional systems [8]**,** and the wave function can be written as a product of a cell periodic part $u_i(\boldsymbol{r})$ and a wavelike part $e^{ik.r}$ with the wave vector **k**,

$$\Psi_j^{(k)}(\boldsymbol{r}+\boldsymbol{R}) = e^{i(k.r)}\Psi_j^{(k)}(\boldsymbol{r}) \quad \textbf{(I.38)}$$

The unit cell periodic part $u_j^{(k)}$ of the wave functions is introduced as:

$$\Psi_j^{(k)}(\boldsymbol{r}) = e^{i(k.r)}u_j^{(k)}(\boldsymbol{r}) \quad \textbf{(I.39)}$$

Where ;

$$u_j^{(r)}(\boldsymbol{r}+\boldsymbol{R}) = u_j^{(k)}(\boldsymbol{r}) \quad \textbf{(I.40)}$$

It means that all cell periodic functions can be written as a sum of plane waves, going to reciprocal space lattice and performing Fourier transform [8]:

$$u_i(r) = \sum_G \boldsymbol{c_i}(\boldsymbol{G})\boldsymbol{e^{iGr}} \quad \textbf{(I.41)}$$

The above some is expanded as a set of finite number of plane waves whose wave vectors are reciprocal lattice vectors of the crystal: $\boldsymbol{e^{i(k.r)}}$ *: are called plane waves; the space of vectors* **r** *is called real space, and the space of vectors* **k** *is called reciprocal space.*

G : are reciprocal lattice vectors chosen by such a way that $\boldsymbol{e^{i(k.r)}}$ has the periodicity of the real space lattice.

So, the electronic wave functions can be written as a sum of plane waves and Fourier transformation, due to the periodicity, becomes a Fourier's series ;

$$\Psi_j^{(k)}(\boldsymbol{r}) = \left(\Omega^{-1/2}\right)e^{iK.r}\sum_G \boldsymbol{c_i}(\boldsymbol{G})\boldsymbol{e^{iGr}} \quad \textbf{(I.42)}$$

$c_i(G)$ **:** represent the expansion coefficients for the plane waves or Fourier coefficient, each have a kinetic energy ($\hbar 2 / 2m)|K + G|^2$.

Then, the electronic wave functions is written as:

$$\Psi_j^{(k)}(r) = \left(\Omega^{-1/2}\right) \sum_G c_i(G) e^{i(G+K)r} \quad \textbf{(I.43)}$$

Where the function of the plane wave basis set is defined as:

$$\emptyset_G(r) = \Omega^{-1/2} e^{iG.r} \quad \textbf{(I.44)}$$

Which are appropriately standardized in the supercell :

$$\langle \emptyset_G | \emptyset_{G'} \rangle = \delta_{G.G'} \quad \textbf{(I.45)}$$

So that the plane wave corresponding to a different wave vectors **G≠ G'.**

The problem of expressing the wave function in terms of an infinite number of reciprocal space vectors of the periodic cell has been mapped by the problem of the infinite number of electrons via the use of Bloch's theorem. This case is treated by sampling the Brillouin zone at special sets of *k*-points.

I. 6.1.Kohn-sham equation in the plane waves basis set :

Another advantage of expanding the electronic wave functions in terms of a basis set of plane waves is that the Kohn-Sham equation **(I.31)** take a particularly simple form[8], and the potential and the kinetic contribution of the Hamiltonian H$\left(H_{G.G'}^k = T_{G.G'}^k + V_{G.G'}^k\right)$ are given by :

$$T_{G.G'}^k = -\frac{1}{2}\langle \emptyset_G^k | \nabla^2 | \emptyset_{G'}^k \rangle = -\frac{1}{2}|K + G|^2 \delta_{G.G'} \quad \textbf{(1.46)}$$

and

$$V_{G.G'} = \langle \emptyset_G^k | \tilde{V} | \emptyset_G^k \rangle = \Omega^{-1} \int V(r) e^{-i(G-G').r} d\,r = \hat{V}(G - G') \quad \textbf{(1.47)}$$

Where :

$\hat{V}(\boldsymbol{G}-\boldsymbol{G}')$ **:** Fourier transformed of the Kohn-sham potential.

So, the equation **(I.31)** becomes :

$$\sum_{G'}\left[\frac{1}{2}|\boldsymbol{K}+\boldsymbol{G}|\delta_{G.G'}+\grave{\boldsymbol{V}}(\boldsymbol{G}-\boldsymbol{G}')\right]\boldsymbol{C_{jk}}(\boldsymbol{G})=\boldsymbol{\varepsilon_{jk}}\boldsymbol{C_{jk}}(\boldsymbol{G}') \qquad \textbf{(1.48)}$$

Usual methods of solving the plane wave expansion of the Kohn-Sham equations is by diagonalisation of the Hamiltonian matrix are given by the term in curly brackets. It follows that the size of the Hamiltonian matrix is determined by the energy cut-off. It is not necessary to solve this by conventional matrix diagonalisation techniques, but a more computationally efficient method exists where the plane wave coefficients are treated as dynamical variables.

I. 6.2. The energy cut-off :

Practically, it couldn't working in infinite base sets **(I.43)**, it must be reduce to a finite size, so what it is too simple for the plane waves by the limitation of the vector set $\vec{\boldsymbol{G}}$ with the condition $\vec{\boldsymbol{G}} < \vec{\boldsymbol{G}}_{\boldsymbol{max}}$, which correspond to a centered radius sphere $\vec{\boldsymbol{G}}_{\boldsymbol{max}}$ in the origin of reciprocal space **(fig.I.1),** means that all the interior vectors of this sphere included in the base set, where the energy associated to the vector $\vec{\boldsymbol{G}}_{\boldsymbol{max}}$ is a specific energy called "cut-off energy" $\boldsymbol{E_{cut}}$.

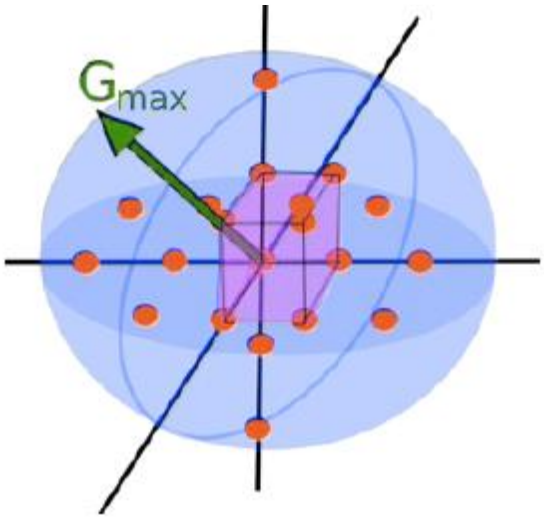

FIG.I.1 : Cut-off energy in reciprocal space **[9].**

The plane waves with a smaller kinetic energy typically have a more important role than those with a very high kinetic energy [5]. Thus, the plane wave basis set can be amputated to include only plane waves that have the kinetic energy less than some particular cut-off energy; this produces the finite basis set :

$$\mathbf{E_{cut}} \geq (\hbar \mathbf{2}\ /\mathbf{2m})|\mathbf{K}+\mathbf{G}|^{2} \qquad \textbf{(I.51)}$$

I. 7. Pseudo-Potentials :

I. 7.1.Pseudo-Potentials concept :

The solution of the Kohn-Sham equations for infinite crystalline systems is now tractable. This is what it has been shown by the use of Bloch's theorem, that a plane wave energy cut-off in the Fourier expansion of the wave function and careful *k*-point sampling. Unfortunately, a plane wave basis set is usually very poorly suited to expanding the electronic wave functions because a very large number are required to accurately describe the rapidly oscillating wave-functions of electrons in the core region. The pseudo-potential approximation introduced as it is well known that most physical properties of solids are dependent on the valence electrons to a much greater degree than that of the tightly bound core electrons. This approximation uses this fact to remove the core electrons and the strong nuclear potential and replace them with a weaker pseudo-potential which acts on a set of pseudo wave-functions rather than the true valence wave-functions. A schematic representation of pseudo-potential method is given in **fig I.2**.

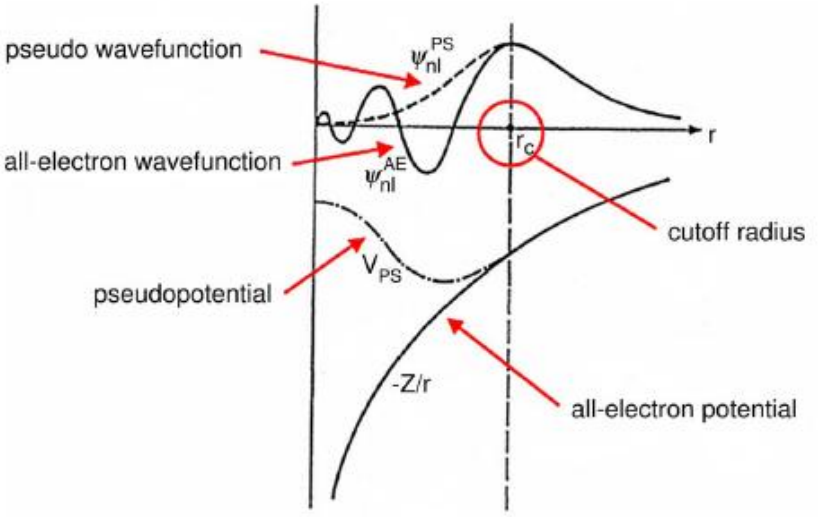

Fig I.2 : The Pseudo-potential approximation**[9]**.

So, generally the fundamental idea behind the pseudo-potential approximation is to 'freeze' the tightly bound core electrons of each atom and replace them with an effective (or pseudo) potential which attenuates the strong Coulomb potential close to the nucleus. The main advantage of removing the core electrons is to relax the orthogonality constraint imposed on the wave-functions of the remaining valence electrons[10]**.**

I. 7.2.The Pseudo-potential theory :

Historically, the first approach to the pseudo-potential was been initially proposed by Fermi (1934) [11] and then by Heilmann (1935) [12], who did append to the electronic structure calculation a considerable simplification. In the end of the years 50th the present approach, first proposed by Phillips et Klein man [13-14], is to construct the pseudo-potential from first principles, starting from a solution to the Schrödinger equation only[15].

Modern pseudopotential methods are inspired, in turn, by the earlier orthogonalized plane-wave method of Herring :

$$\emptyset_{OPW}(\boldsymbol{K}+\boldsymbol{G}) = \emptyset_{PW}(\boldsymbol{K}+\boldsymbol{G}) - \sum_{\alpha.c}\langle\varphi_c|\emptyset_{PW}(\boldsymbol{K}+\boldsymbol{G})\rangle\varphi_{\alpha.c} \qquad \textbf{(I.49)}$$

where $\emptyset_{PW}$ is the plane wave.

I. 7.2.1. Norm-Conserving Condition :

Norm conserving pseudo-potentials are developed under the following conditions [6]:

1. Real and pseudo valence-state eigen-values are the same for a selected atomic configuration. :

$$\varepsilon_l^{PP} = \varepsilon_{nl}^{AE} \quad \textbf{(I.50)}$$

2. Real and pseudo-wave functions (PP) and all electrons (AE) are equal must be matched beyond a core radius r_c

$$R_l^{PP}(r) = R_{nl}^{AE}(r), \qquad if \ r \geq r_c \quad \textbf{(I.51)}$$

3. The first energy derivative of the logarithmic derivatives of the real and pseudo wave functions agree at $r \geq r_c$.

4. The integrals from 0 to r of the real and pseudo-charge densities agree for each valence state for $r < r_c$. Thus both charge densities should be equal beyond the core radius. That is means in the interior of r_c ($r > r_c$) the pseudo wave functions norms and all electrons are equal :

$$\int_0^{r_c} dr|rR_l^{PP}(r)|^2 = \int_0^{r_c} dr\left|rR_{nl}^{AE}(r)\right|^2 \ , \ si\ r < r_c \quad \textbf{(I.52)}$$

5. The logarithmic derivatives of the real and pseudo-wave functions agree at r_c .

I. 7.2.2.Ultrasoft Pseudo-potentials :

An ultrasoft pseudopotential was developed by Vanderbilt (1990) to achieve a much smoother pseudo-wave function [6]. It's a new pseudo-potentials class characterized by the pseudo wave function arbitrarily smooth in the core region for this raison it named "**Ultrasoft Pseudo-potentials"**. This method is based on two main points :

1) The potentials are constructed from the atomic states evaluated at two different energies. It means that more than one reference energy per quantum state is allowed. Usually these are not used in calculation.

2) Dropping the norm-conservation constraint leads to a new class of pseudo-potentials. The pseudopotential operator is no longer Hermitian; but it is possible to transform the standard eigenvalue form to a generalized eigenvalue problem.

This approach has a number of advantages, for example; the same exchange and correlation functional for atomic and solid state calculations can be used. It is possible to generate softer and harder potentials by changing the core radius.

BIBLIOGRAPHY :

[1] T. Bhattacharjee. Towards Understanding Catalytic processes for the Reactivity of Hydrocarbons on Rh Surface: A Quantum Chemical Study. PhD Thesis, Heidelberg University, 2011.

[2] J. D. Cresser. Wave Mechanics Notes for PHYS201. Macquarie University, Sydney. 2005 (42).

[3] M. Born and J.R. Oppenheimer. Ann. Phys. **87** (1927) 457.

[4] D. CHERRAD. Étude *Ab initio* des propriétés structurales, élastiques, électroniques et optiques des perovskites CaXO3 (X=Sn et Hf) dans la phase cubique et orthorhombique Thèse Doctorat ès Science, Université Ferhat Abbas de Sétif, 2012.

[5] R. M. A. KHALIL. Ab initio studies of the structural, dynamical and thermodynamical properties of graphitic and hydrogenated graphitic materials and their potential for use in hydrogen storage. PhD Thesis, University of Salford, Salford, UK.2014.

[6] V. Fock. Z. Physik 61 (1930) 126.

[7] S; tClark,, Density functional theory. Phd thesis, Durham University, UK 1996.

[8] W. Kohn and L. J. Sham. Phys. Rev. 140, (1965) A1133.

[9] C. François-Xavier. DFT with plane waves, pseudopotentials, Tutoriel CPMD/CP2K Paris, 6–9 avril. 2010.

[10] F. Corsetti. On the properties of point defects in silicon nanostructures from ab initio calculations. PhD Thesis, Imperial College London, 2012.

[11] E. Fermi, Il Nuovo Cimento 11, (1934) 157.

[12] H. Hellmann, J. Chem. Phys. 3 (1935) 61.

[13] J. C. Phillips and L. Kleinman, Phys. Rev. 116 (1959) 287.

[14] E. Antončík, J. Phys. Chem. Solids 10 (1959) 314.

[15] B. Tegner. Phase Stability of Titanium Alloys :A First Principles Study. PhD Thesis,The University of Edinburgh, 2014.

CHAPTER II :

CASTEP code

CHAPTER II :

CASTEP code

II 1. CASTEP code preview :

CASTEP code (CAmbridge Serial Total Energy Package), developed by Clark et al. [1], is a software package and first principal quantum mechanical ab initio code aiming to perform electronic structure and any physical properties calculations using density functional theory with plan waves basis set. It is fully featured first principal code and as such its capabilities are numerous[2]:

- It can be used to simulate a wide range of materials including solids, surface, molecules…
- Possibly finite temperature molecular dynamics and perform full geometry optimization.
- It can impose symmetry and constraints (both internal and external to the cell) in the calculations, either as defined by the user, or automatically using in-built symmetry detection.
- It performs a variational solution to the Kohn-Sham equations by using a density mixing scheme and conjugate gradients to minimize the total energy and relax the ions under the influence of the Hellmann-Feynman forces, respectively.
- It reduces the computational cost and memory requirement for operating with the Hamiltonian on the electronic wavefunctions and provides an efficient way of transforming various entities (wave functions, potentials) from real to reciprocal space using fast Fourier transforms (FFT).

Two algorithms SCF (Self-consistent Field) are implemented in the CASTEP code to determine the electronic ground states of system. First, density Mixing (DM) [3], it is generally faster and is not variational. This leads to instability of convergence. In this

algorithm, the sum of the eigenvalues is minimized, based on the conjugate gradient-approach, instead of the self-consistent minimization of the total energy. The new electron density (ρ_{out}) is mixed with the initial density (ρ_{in}) and the process repeats until the convergence is reached. CASTEP supports, in increasing order of robustness, four mixing methods: linear mixing, Kerker mixing, Broyden mixing, and Pulay mixing. The density-mixing technique converges for both insulators and metals. Second, all bands / EDFT [4], it is variational but is generally slower. In addition, it involves the minimization of total energy using the preconditioned conjugate gradient technique [5]. The choice of one or the other algorithm is governed by the convergence difficulties of CASTEP for a given system.

The electron-ion potential is described using ab initio pseudopotentials (norm-conserving and ultra-soft). Energy minimization procedures are used to obtain the electronic wave functions and the corresponding charge density. CASTEP uses the Monkhorst-Pack method for sampling the Brillouin zone [6].

The determination of the optimized structure of a given system requires the calculation and then the minimization of the forces applied on each atom that constitutes such system. These forces are obtained by the Hellmann-Feynman theorem [7]. The total Hamiltonian of the system depends parametrically on positions of nucleus $\boldsymbol{R_I}$. The force applied on each atom is: given as:

$$F_I = -\frac{\partial E}{\partial \boldsymbol{R_I}} = \left\langle \Psi \middle| -\frac{\partial \hat{H}}{\partial \boldsymbol{R_I}} \middle| \Psi \right\rangle = \int d^3\boldsymbol{r}\rho(r)\frac{Z_I(\boldsymbol{r}-\boldsymbol{R_I})}{|\boldsymbol{r}-\boldsymbol{R_I}|} + \sum_{J\neq I} Z_I Z_J \frac{(\boldsymbol{R_I}-\boldsymbol{R_J})}{|\boldsymbol{R_I}-\boldsymbol{R_J}|^3} \quad (3.1)$$

This equation can be used to find the equilibrium geometry of a molecule or solid by varying all positions $\boldsymbol{R_I}$ until the energy is minimal and its derivative is equal to 0 (the configuration of the nuclei for which all forces and constraints are zero). Thus, the Hellmann-Feynman method opens the possibility of finding the equilibrium position of the nuclei (as well as the equilibrium lattice parameters). In this work, geometry optimization is carried out in a self-consistent method within BFGS algorithm (Broyden, Fletcher, Goldfarb and Shannon), which allows to optimize a cell in the presence of external constraint from a chosen configuration until the desired convergence criteria are reached.

The energy gap (difference between energy values of the higher valence band and the lower conduction band) can provide insight in potential uses for optical device applications. However, the energy gap calculated from the Kohn-Sham eigenvalues (DFT)

using the LDA and GGA methods is underestimated with respect to the energy gap obtained experimentally (from 50% to 100%) [8].

II 2. Delafossite structure of 2H-$CuGaO_2$:

The unit cell and the Brillouin zone with high symmetry k-points in reciprocal space for the delafossite structure of 2H-$CuGaO_2$ compound are shown in figure (II.1). The crystallographic construction of this structure has been obtained by using the complementary module of visualization of structures implemented in software *'Materials Studio. v5.5 '* commercialized by *'*Accelery. Inc*'*.

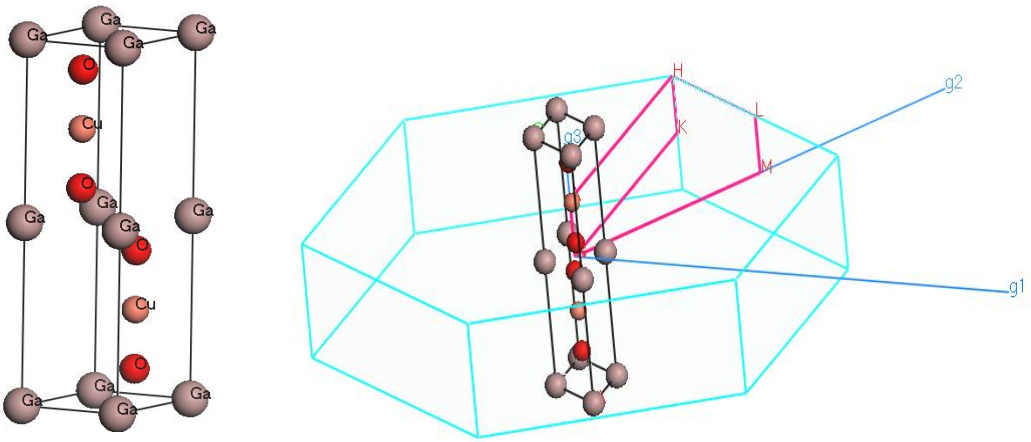

***Figure II*. 1 :** The unit cell and the Brillouin zone of the delafossite structure for 2H-$CuGaO_2$ compound (**g1**, **g2** and **g3** are the reciprocal lattice vectors).

II 3. Electronic density of charges :

The electronic density of charges is given by the following expression:

$$\rho(\vec{r}) = \frac{(2\pi)^3}{\Omega} \int_{BZ} d\vec{k} \sum_i f_{ik} [\rho_i(k)]^2 \qquad \text{(II.2)}$$

The sum is done on the occupied orbitals and the integral extends over the first Brillioun zone. So, a large number of k-points is necessary to describe precisely the large number of free electrons in a metal. On the contrary, we can predict the total energy in insulatrs and semiconductors with a small number of points [9].

II 4. Monkhorst and Pack special points :

Monkhorst and Pack (1976) [6], described the method consisting a set of special k-points for selecting the appropriate sampling of Brillouin zone. A uniform grid of a k-points has been produced by the authors along the three axes in the reciprocal space.

The Monkhorst and Pack grid is defined by three integers which indicates the division number along each axe. These integers generate a sequence of numbers as follows:

$$U_r = \frac{(2r - q_i - 1)}{2q_i} \qquad \text{(II.3)}$$

Where r varies between 1 and $\boldsymbol{q_i}$ that i = 1, 2 et 3.

The Monkhorst and Pack grid is obtained from these sequences :

$$\boldsymbol{K}_{prs} = u_p \boldsymbol{g}_1 + u_r \boldsymbol{g}_2 + u_s \boldsymbol{g}_3 \qquad \text{(II.4)}$$

$\boldsymbol{g_i}$: represents the vectors basis in the reciprocal lattice.

For the hexagonal systems [10], the points are amended along the axes of $\boldsymbol{g}_1$ and $\boldsymbol{g}_2$:

$$U_p = \frac{(p-1)}{q_i} \qquad \text{(II.5)}$$

(P takes values between 1 and $\boldsymbol{q_i}$)

II 5. Mulliken population :

Sanchez-Portal et al [11], described a technique to carry the population analysis in CASTEP code by means of a projection of the plane wave states on a localized basis. Subsequently, The analysis of the population of the resulting projected states is then carried out using the Mulliken formalism [12]. The charge associated with a given atom, A, is determined by:

$$Q(A) = \sum_K w_K \sum_\mu \sum_v 2P_{\mu v}(k) S_{v\mu}(k) \quad \text{(II.6)}$$

Where:

$S_{v\mu}(k) = \langle \Phi^\mu(k) | \Phi^v(k) \rangle$:is the overlap matrix ,

$P_{\mu v}(k) = \langle \Phi^\mu(k) | \rho(k) | \Phi^v(k) \rangle$: is the density matrix,

$w_{\alpha\mu}(k) = \langle \Psi^\alpha(k) | \Phi^\mu(k) \rangle \langle \Phi^\alpha(k) | \Psi^\alpha(k) \rangle$: is the band weight α on the orbital μ.

II 6. Electronic density of states:

The density of states (DOS) counts the number of electronic states having a given energy. For a band n, the density of states is given by:

$$N_n(E) = \int \frac{\delta(E - E_n(k))}{4\pi^3} d\boldsymbol{k}$$

(II.7)

The integral extends over all the Birillioun zone .

The total density of states $N(E)$ is obtained by summation on all bands n :

$$N(E) = \sum_n \int \frac{\delta(E - E_{k.n})}{4\pi^3} d\boldsymbol{k}$$

(II.8)

A linear interpolation diagram developed by Auckland [13], in the parallelepipeds formed by Monkhorst-Pack points was used by the CASTEP code.

II 7. Elasticity constants :

II 7. 1. Monocrystals - anisotropic elasticity:

In the elastic region where the constraint is less than a certain limit value and the deformation will be temporary, the crystal returns to its original form once the constraint is removed, the deformation on a solid is then linearly proportional to the magnitude of the

applied stress. This law, demonstrated by the english scientist Robert Hook in 1678 and generalized after that by Cauchy (1787-1857), proposed to express every component of constraint tensor σ as a linear function of deformation tensor one ε as :

$$\sigma_i = C_{ij}\varepsilon_j \qquad \text{(II.9)}$$

Or reciprocally;

$$\varepsilon_i = S_{ij}\sigma_j \qquad \text{(II.10)}$$

Where i, j=1,..6 (Voigt notation) and C (C_{ij} elements) and S (S_{ij} elements) are the elasticity tensor (also called stiffness tensor) and compliance tensor (flexibility), respectively. These two tensors are symmetric with 21 independent elastic constants for a totally anisotropic material which presents no symmetry operation and they have only two independent elastic constants C_{11} and C_{12} for isotropic material..

For the hexagonal II system of the space group P63/mmc, the elastic constants matrix takes the following form:

$$\begin{pmatrix} C_{11} & C_{12} & C_{13} & 0 & 0 & 0 \\ 0 & C_{11} & C_{13} & 0 & 0 & 0 \\ 0 & 0 & C_{33} & 0 & 0 & 0 \\ 0 & 0 & 0 & C_{44} & 0 & 0 \\ 0 & 0 & 0 & 0 & C_{44} & 0 \\ 0 & 0 & 0 & 0 & 0 & \frac{1}{2}(C_{11}-C_{12}) \end{pmatrix} \qquad \text{(II.11)}$$

The determination of the elasticity constants from the DFT calculations is by fixing the constraint (deformation) to a finite value, optimizing all the free parameters of the structure and then calculating the deformation (the constraint) from the relation (II.9).

II 7. 2.Polycristals- isotropic elasticity :

Most materials, which are produced in polycrystalline form, have a large dimension compared with those of the microcrystals. Generally, the macroscopic isotropy of material

results from an average of anisotropic properties of many microcrystals and the elastic properties do not depend on the orientation within the material.

The elastic behavior of a polycrystalline system is described only by two elastic constants; Young's modulus (or rigidity) E and Poisson's ratio η, bulk modulus B and shear modulus G or the two Lamé's constants (λ and μ) [14].

In the general case, the uniaxial rigidity of a solid or the solid resistance to the uniaxial deformation is characterized by the Young's modulus defined by :

$$E_{ii} = \sigma_{ii}/\varepsilon_{ii} \qquad \text{(II.12)}$$

Thus, the Poisson's coefficient, characterizes the shrinking along the axis perpendicular to the direction of the stress, is given by the following expression:

$$\eta_{ij} = -\varepsilon_{ii}/\varepsilon_{jj} \qquad \text{(II.13)}$$

Furthermore, the deformation divided into bulk modulus B (volume changing under constant form) and shear modulus G (form changing under constant volume). These tow parameters are given by :

$$B = V\frac{d^2U}{dV^2} \qquad \text{(II.14)}$$

and

$$\tau = G\gamma \qquad \text{(II.15)}$$

where :

U : is the energy of unit cell in volume V and $\gamma = 2\varepsilon_d$ is the shear deformation.

The four elastic modulus B, G, E and η interconnected themselves by the following relation :

$$E = \frac{9BG}{3B+G} \quad \text{and} \quad \eta = \frac{3B-2G}{2(3B+G)} \qquad \text{(II.16)}$$

Or reciprocally,

$$B = \frac{E}{3(1-\eta)} \quad \text{and} \quad G = \frac{E}{3(1+\eta)} \tag{II.17}$$

The polycrystalline material is consist of monocrystalline grains each has its own crystalline orientation. This implies that each grain responds differently to the applied stress. The different responses in the polycrystalline solid are then averaged. Different methods have been proposed in order to calculate the elastic properties of polycrystalline phases.

In the Voigt hypothesis case [15], the deformation is assumed to be constant throughout the polycrystalline and equals to the macroscopic deformation applied on the sample. This returns to take an average on the elastic modulus C_{ij} over the entire space of orientations. Moreover, in the Reuss's hypothesis [16] the constraint assumed to be constant throughout the polycrystalline and equals to the microscopic constraint. The average taken on the deformability coefficient S_{ij}. The compressibility modulus and shear's modulus in these two approaches are given by:

$$B_V = \frac{1}{9}[2(C_{11} + C_{12}) + C_{33} + 4C_{13}]$$

$$G_V = \frac{1}{5}\left(G_{eff}^V + 2\mu_1 + 2\mu_2\right)$$

$$B_R = \frac{(C_{11}+C_{12})C_{33}-2C_{13}^2}{6G_{eff}^r}$$

$$G_R = \left[\frac{1}{5}\left(\frac{1}{G_{eff}^r} + \frac{2}{\mu_1} + \frac{2}{\mu_2}\right)\right]^{-1} \tag{II.18}$$

With

$$G_{eff}^V = \frac{1}{3}(C_{11} + C_{33} - 2C_{13} - C_{66})$$

$$G_{eff}^r = \frac{(C_{11}+C_{12})C_{33}-2C_{13}^2}{6B_V}$$

$$\mu_1 = \frac{1}{2}\left\{C_{44} + C_{66} + [(C_{44} - C_{66})^2 + 4C_{14}^2]^{1/2}\right\}$$

$$\mu_2 = \frac{1}{2}\{C_{44} + C_{66} - [(C_{44} - C_{66})^2 + 4C_{14}^2]^{1/2}\} \quad \text{(III.19)}$$

In the Hill's hypothesis [17] the modulus of a polycrystalline solid is necessarily between the those of Voigt and Reuss.

The elasticity modulus *B* and *G* are approximated by Hill's average, which is given by:

$$B^{Hill} = (B^{Voigt} + B^{Reuss})/2 \text{ and } G^{Hill} = (G^{Voigt} + G^{Reuss})/2 \quad \text{(II.20)}$$

For an isotropic system the elasticity matrix and suppleness constants reduce to the following forms:

$$\begin{bmatrix} C_{11} & C_{12} & C_{12} & 0 & 0 & 0 \\ . & C_{11} & C_{12} & 0 & 0 & 0 \\ . & . & C_{11} & 0 & 0 & 0 \\ . & . & . & \frac{C_{11}-C_{12}}{2} & 0 & 0 \\ . & . & . & . & \frac{C_{11}-C_{12}}{2} & 0 \\ . & . & . & . & . & \frac{C_{11}-C_{12}}{2} \end{bmatrix} \quad \text{(II.21)}$$

$$\begin{bmatrix} S_{11} & S_{12} & S_{12} & 0 & 0 & 0 \\ . & S_{11} & S_{12} & 0 & 0 & 0 \\ . & . & S_{11} & 0 & 0 & 0 \\ . & . & . & 2(S_{11}-S_{12}) & 0 & 0 \\ . & . & . & . & 2(S_{11}-S_{12}) & 0 \\ . & . & . & . & . & 2(S_{11}-S_{12}) \end{bmatrix} \quad \text{(II.22)}$$

Furthermore, shear's modulus, Young's modulus, Poisson's coefficient and Lamé's constants, are written, respectively, as follows:

$$G = \frac{1}{2(S_{11}-S_{12})} = \frac{1}{S_4} \quad \text{(II.23)}$$

$$E = \frac{1}{S_{11}} \tag{II.24}$$

$$\eta = -\frac{S_{12}}{S_{11}} \tag{II.25}$$

$$u = C_{44} = \frac{1}{2}(C_{11} - C_{12}) = \frac{1}{S_{44}} = G,\ \lambda = C_{12} \tag{II.26}$$

II 8.Calculation setting:

In the present calculation we use the generalized gradient approximation of Perdew and al (GGA-PW91)[18] to evaluate of the exchange-correlation functional. Also, to describe the electron-ion interaction, we use the ultrasoft pseudo-potential of Vanderbilt extracted from the material studio library (Accelrys ©). In addition, the considered valence stats for the different atoms of the studied material are given as: O $2s^2\ 2p^4$, Cu $3d^{10}\ 4s^1$, Ga $3d^{10}\ 4s^2\ 4p^1$.

The convergence criteria used here are :

- ✓ maximal forces is : 0.01 eV/Å.
- ✓ energy is: 5.0 10^{-6} eV/atome.
- ✓ maximum displacemant is : 5.0 10^{-4} Å.
- ✓ maximum stress is : 0.02 GPa.

- The size of the plane wave basis set is fixed by the choice of the cutoff energy: a convergence test series lead us to choose *Ecut*= 380 eV. This value has been assisted by using ultrasoft pseudo-potential which allows to reduce the cutoff energy compared to that used in the norm-conserving pseudo-potential [14].
- The sampling of the first Brillouin zone has been realized by using 14 k-points which corresponds to Monkhrost-Pack points set 10×10×2. These values are chosen after a convergence test series on the desired precision.

Bibliography:

[1] S. J. Clark, M. D. Segall, C. J. Pickard , P. J. Hasnipm, M. I. J. Probert , K. Refson and M. C. Payne, Z. Kristallogr. 220 (2005) 567.

[2] R .Mahlangu, First principle study of Ti-Al and Pt-Ti ALLOYS, Master thesis, UNIVERSITY OF LIMPOPO-Turfloop Campus, 2009.

[3] G.Kresse, J. Furthmuller, Phys. Rev. B, 54 (1996) 11169.

[4] N. Marzari, D. Vanderbilt, M. C. Payne, Phys. Rev. Lett. 79 (1997) 1337.

(1939) 340.

[5] M.C. Payne, M.P. Teter, D.C. Allan, T.A. Arias and J. D. Joannopoulos, Rev. Mod. Phys. 64 (1992) 1045.

[6] H. J. Monkhorst and J. D. Pack. Phys. Rev. B 13 (1976) 5188.

[7] R. Feynman, Phys. Rev. 56 (1939) 340.

[8] R. Besma, Etude des propriétés structurales, électroniques, optiques et élastiques du composé 3R-CuGaO2. Mémoire de Master, Université M^{ed} Boudiaf, M'sila-Algérie. 2016.

[9] DJ. Cherrad. Thèse Doctorat ès Science. Étude Ab initio des propriétés structurales, élastiques, électroniques et optiques des perovskites CaXO3 (X=Sn et Hf) dans la phase cubique et orthorhombique. Univ. Ferhat Abbas de Sétif, 2002.

[10] H. J. Monkhorst, J. D. Pack, Phys. Rev. B 16 (1977) 1748-1749

[11] D. Sanchez-Portal, E.Artacho, J. M. Soler, Solid State Commun., **95**, 685-690 (1995).

[12] Mulliken, R. S. J. Chem. Phys., **23**, 1833-1846 (1955).

[13] G. J. Ackland, Phys. Rev. Lett., 80 (1998) 2233.

[14] Kh. Haddadi. Etude des propriétés structurales, élastiques et électroniques des composés antiperovskites de type XNCa3.Thèse Doctorat ès Science. Univ. Ferhat Abbas de Sétif, 2013.

[15]. W. Voigt, Lehrburch der Kristallphysik. Leipzig: Teubner; 1928.

[16] A. Reuss, Angew Z. Math. Mech. 9 (1929) 49.

[17] R. Hill, Proc. Phys. Soc. London 65 (1952) 396.

[18] J. P. Perdew, J. A. Chevary, S. H.Vosko, K. A. Jackson, M. R. Pederson, D. J. Singh, C. Fiolhais, Phys. Rev. B, 46 (1992) 6671.

CHAPTER III:

Results & discussion

CHAPTER III:

Results & discussion

Introduction :

$CuGO_2$ belongs to the delafossite structure with the general formula **ABO_2**. It has a hexagonal structure (space group number : 194; Hermann-Mauguin symbol: $P63/MMC$; Schoenflies symbol: D_{6H}^4) described by $a = b$, c , $\alpha = \beta = 90°$ et $\gamma = 120°$ as shown in $\boldsymbol{figure(III.1)}$

- In this structure the gallium (**Ga)** and the copper (**Cu)** atoms take the Wyckoff positions which are (2a) (0,0,0) and (2c) (1/3,2/3,1/4), respectively. The position of the oxygen atom (O) is at (4f) site (1/3,2/3,***u***), where ***u*** is an intern parameter .

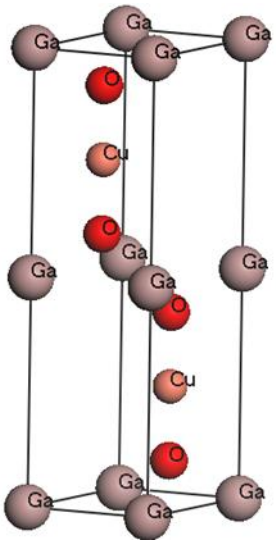

***Figure*(*III*.1):** The structure of the hexagonal delafossite unit cell for the compound **2H-$CuGaO_2$.**

III. 2. The structural properties :

We calculated the lattice parameters of the **$CuGaO_2$** under **P= 0 GPa** . The geometry optimization results of this material are performed with the plane wave ultrasoft pseudo-

potential using the generalized gradient approximation (GGA) with the PW91 functional as implemented in CASTEP code [1],and are presented in the ***table*(*III*. 1)**

***Table*(*III*. 1):** Calculated lattice parameter *a=b, c and interatomic distance d* with the available experimental and theoretical values.

Parameter	Present work	Theoritical value	Experimental value
***a=b* (A°)**	3.0248	2.9730[a], 2.973[b] , 2.913[b], 2.931[b], 2.942[c], 3.0110[c], 3.0260[d]	2.9730[e]
***c*(A°)**	11.5594	11.5950[a], 11.595[b], 11.455[b], 11.340[b], 11.3248[c], 11.4409[c], 11.5609[d]	11.5950[e]
u	0.4118		
d_{Cu-O} (A°)	1.8706	1.8707[d]	
d_{Ga-O} (A°)	2.0221	2.0228[d]	
d_{O-O} (A°)	2.6842	2.6852[d]	

a [2], b [3], c [4]. d[5], e[6]

- This table gives available theoretical and experimental data of the lattice parameter values and *interatomic distance d* of our compound.
- It is well known that in general the GGA overestimates the structural parameters, whereas the LDA underestimates them. From reported values in the above table, it's clear that, in general, our calculated values are close to the existing theoretical and experimental results: the deviation of the obtained results for the lattice parameter ***a* = *b*** (***c***) with respect to the theoretical results is ranging from 1.74% to 0.04% (0.31% to 0.02%), whereas it is of the order of 1.74% (0.31%) relative to other experimental results.

III. 3. Electronic properties :

III. 3.1. Electronic band structure :

In order to analyze the electronic properties we represent, in $\boldsymbol{figure(III.2)}$, the electronic band structures and the corresponding total density of states (TDOS) diagram of 2H-$\mathbf{CuGaO_2}$ compound along high symmetry lines of the first Brillioun zone, under equilibrium condition performed by the geometry optimization in the previous section.

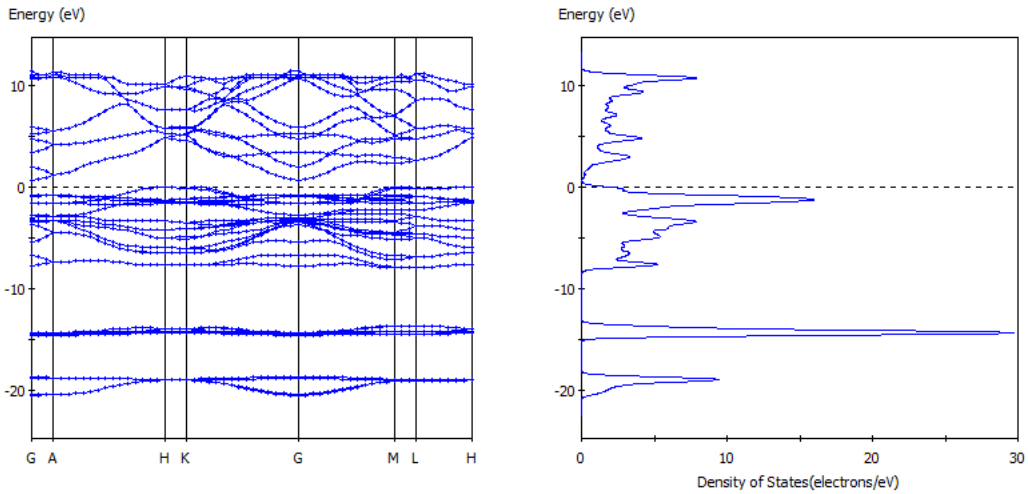

$\boldsymbol{Figure(III.2)}$**: B**and structures and total density of states (TDOS) of 2H-$\mathbf{CuGaO_2}$**.**

The Fermi level $\boldsymbol{E_F}$ is chosen to be 0 eV (dotted horizontal line). It's located at the maximum of the valence band. By definition, the difference between the maximum of the valence band and the minimum of the conduction band is the fundamental energy gap for insulators materials (semiconductor or dielectric material) [8].

Also, band structures illustrated in $\boldsymbol{figure(III.2)}$ allows us to evaluate the values of the direct and indirect band gaps($\boldsymbol{table(III.2)}$).

We note that :

- The valence band maximum (VBM) is located at **H** point**.**
- The conduction band minimum (CBM) is located at **G** point.

Therefore , this compound has an indirect band gap (**G -H**) about 0.715 eV.

***Table*(*III*.2):** Calculated indirect and direct energy band gaps (eV) of 2H-**$CuGaO_2$**.

Direct		Indirect									
G-G	1,489	G-A	1,51	A-H	1,284	H-K	4,896	K-M	4,604	M-L	2,384
A-A	2,079	G-H	0,715	A-K	1,325	H-M	4,899	K-L	4,646	L-G	3,445
H-H	4,896	G-K	0,756	A-M	1,287	H-L	4,941	M-G	3,113	L-A	3,466
K-K	4,642	G-M	0,718	A-L	1,329	K-G	5,375	M-A	3,134	L-H	2,671
M-M	2,342	G-L	0,76	H-G	5,67	K-A	5,396	M-H	2,339	L-K	2,712
L-L	2,716	A-G	2,058	H-A	5,691	K-H	4,601	M-K	2,38	L-M	2,674

***Table*(*III*.3):** Calculated energy band gaps for 2H-**CuGaO2** with the available experimental and theoretical values for comparison.

Energy band gap	Present work	Theoretical	Experimental
Indirect (H-G)	**0,715**	0.708[d]	0.85[a]
Direct (G-G)	1,489	1.483[d]	3.4[e], 3.6[f]

a [2], d [5], f [7], g [8]

The values reported in the above table are underestimated by those of the experiment. This can be interpreted by the fact that at ambient temperature the vibrations of the structure are not taken into consideration. Moreover, the resolution of the Schrödinger equation does not take into account the spin-orbit interaction. In addition, the GGA approximation generally underestimates the energy band gaps because it is not flexible enough to obtain the exact shape of the exchange-correlation potential [9].

Moreover, our values of energy band gap are closer to theoretical values, which are also calculated in the frame work of the DFT. The deviation of the indirect band gap compared to

the experimental result is of the order of 1.58% whereas it is ranging from 0.56% to 0.58% for direct band gap.

III. 3.2.Density of states :

Figure(**III. 3**) exhibits the total (TDOS) and the partial (PDOS) density of states of delafossite compound 2H-**$CuGaO_2$.** We observe that the total density of states (TDOS) can be divided into two parts separated by the fundamental gap.

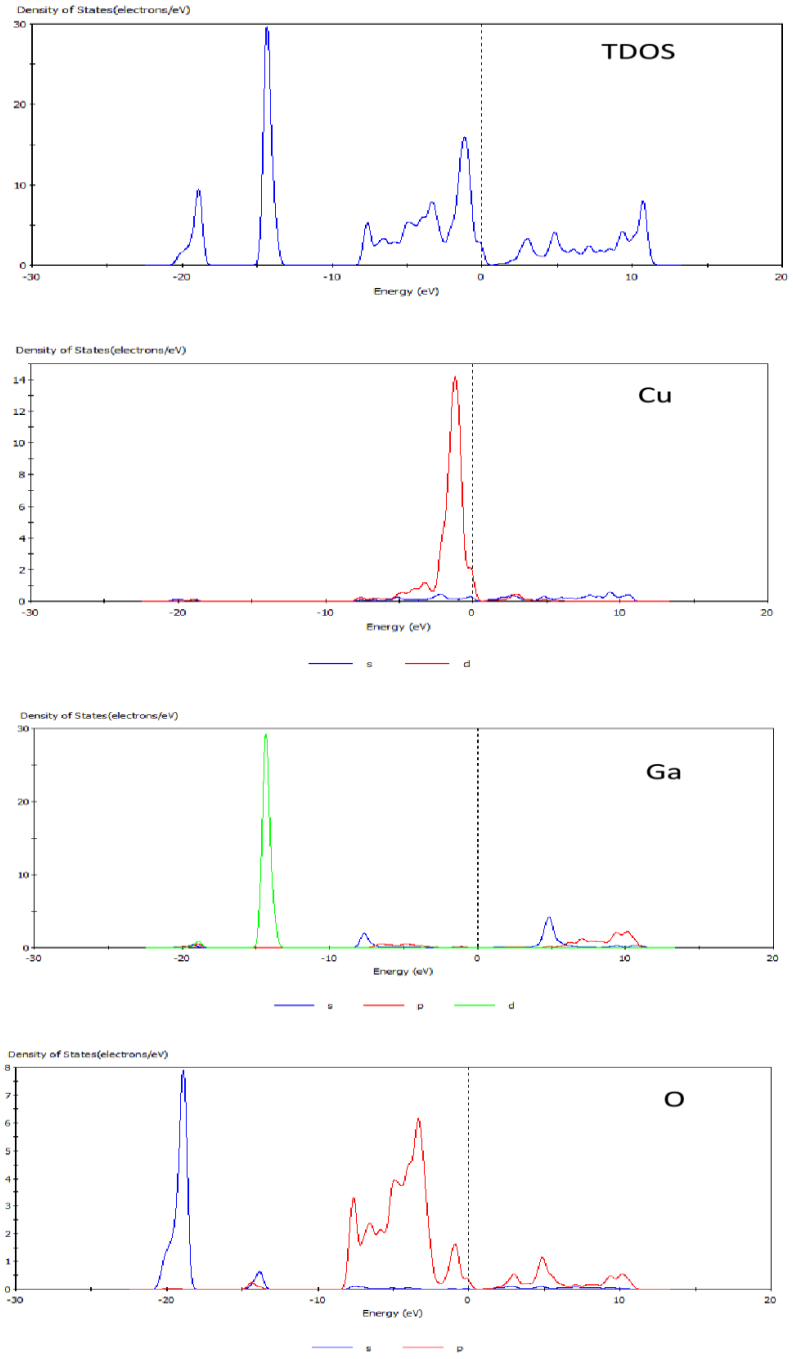

***Figure*(*III*.3) :**The total (TDOS) and partial (PDOS) density of states of 2H-**$CuGaO_2$.**

Also, we can see that the O 2s electronic states are predominant in the lower valence bands. The DOS in the middle valence bands is mostly composed of Ga 3d electronic states with some mixture of O 2s states. The upper valence bands are mainly composed of O 2p and Cu 3d states.

III. 3.3. Mulliken's population analysis:

In the end of the determination and exploring the nature of chemical bonds between atoms using the charge density distribution associated with valence states in the framework of Mulliken's population analysis by calculating the transferred charges between the cations and the anions.

***Table*(*III*.3)** gathers the results of the orbital's partial charges and the total charge for each atom and the transferred charge between atoms of our compound CuGaO2.

***Table*(*III*.3):** Calculated Mulliken partial, total and transferred charges.

Species	Ion	s(e)	p(e)	d(e)	f(e)	Total	Charge (e)
O	1-4	1.85	4.95	0.00	0.00	6.80	-0.80
Cu	1-2	0.71	0.55	9.65	0.00	10.91	0.09
Ga	1-2	0.49	1.01	10.00	0.00	11.50	1.50

The table indicates that ;

- ✓ Each O atom receives 0,8 e from the total charge transferred by the tow other atoms Cu (0.09 e) and Ga (1.50 e).

- ✓ The transfer of charge is caused by the difference of the electronegativity of constituent atoms of **$CuGaO_2$** (3.5 :O, 1.8 ; Cu et 1.8 ; Ga).
- ✓ Thereby , the considered material has a valence states $Cu^{+1}Ga^{+3}O^{-2}$
- ✓ Effective valence states suggested via the calculations results $Cu^{+0.09}Ga^{+1.50}O^{-0.8}{}_2$.

Accordingly, the **$CuGaO_2$** bonds, shown in ***figure*(*III*.4),** are not purely ionic ; the ionic character may be estimated from the effective ionic valence, which is defined by the difference between the formal ionic charge and the Mulliken charge [10]. A zero value indicates a purely ionic bond, while values greater than zero indicate increasing levels of covalence (The effective ionic valence for Cu is 0.91(e) and for Ga is 1.50(e)).

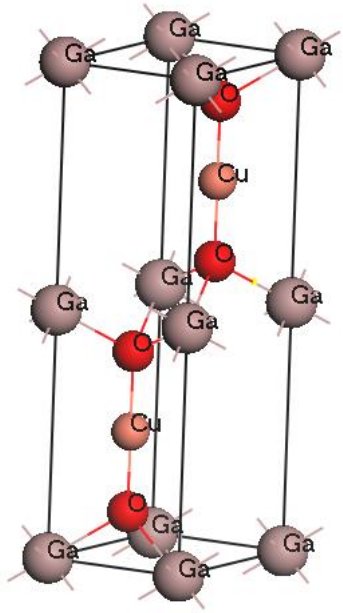

***Figure*(*III*.4):** Unit cell presents the chemical bonds in the compound 2H-$CuGaO_2$

III. 3.4. Charge density of valence electrons :

***Figure*(*III*.5)** presents the charge density distribution from $(11\bar{2}0)$ plane of $CuGaO_2$. This distribution allows us to explore the nature of chemical bonding between atoms. From this figure, we observe that there is an interaction between the charges of Ga and O on the one

hand and between those of Cu and O on the other hand. The density of electronic charges is slightly asymmetric for both bonds. So, the large transfer of charges from the cation to the anion indicates that the anion (O^{-2}) has a higher electronegativity than that of the cation (Cu^{+1} and Ga^{+3}). The high ionic valence of Cu (0.91 e) compared to Ga (1.50 e) indicates that the Cu-O bond is much more covalent than the Ga-O bond. This latter has a coexistence between the ionic and covalent bonds.

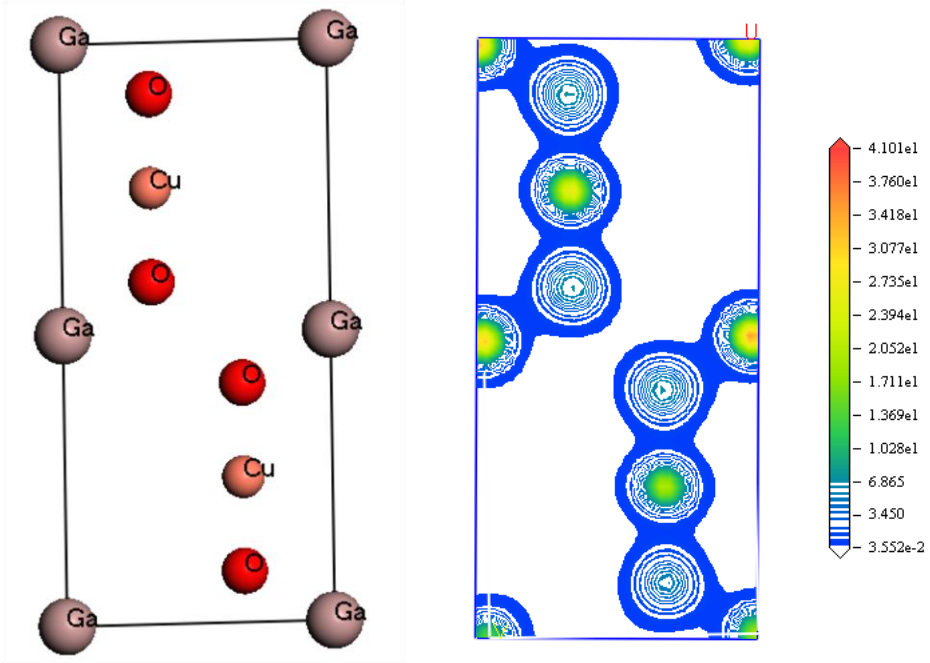

***Figure*(*III*. 5):** Charge density distribution *(e/A*^{3}) from (11$\bar{2}$0) plane of $CuGaO_2$.

III. 4. Optical properties :

The optical properties of a material allow us to study the characteristics of the light passing through it by modifying its vector and/or propagation intensity. In this section the optical properties of $CuGaO_2$ compound are discussed in terms of dielectric function and absorption coefficient [11].

III. 4.1. Dielectric function :

Dielectric function ε (ω) is indispensable to describe the behavior of semiconductors undergoes to the effect of external light excitation. This function is complex and it's written as :

$$\varepsilon(\omega) = \varepsilon_1(\omega) + i\varepsilon_2(\omega) \qquad \text{(III.1)}$$

where $\varepsilon_2(\omega)$ is the imaginary part given as [11] :

$$\varepsilon_2(\omega) = \frac{8}{3\pi\omega^2}\sum_{nn'}\int_{BZ}|P_{nn'}(K)|^2\frac{dS_K}{\nabla\omega_{nn'}(K)} \qquad \text{(III.2)}$$

$P_{nn'}(K)$: elements of the dipole matrix between the initial state $|nk\rangle$ with energy $E_n(k)$ and the final state $|nk'\rangle$ with energy $E_{n'}(k)$.

S_k : Equienergy surface and $\omega_{nn'}(k) = E_n(k) - E_{n'}(k)$.

The real part $\varepsilon_1(\omega)$ of the dielectric function $\varepsilon(\omega)$ can be derived from the imaginary part as :

$$\varepsilon_1(\omega) = 1 + \frac{2}{\pi}P\int_0^{\infty}\frac{\omega'\varepsilon_{2(\omega')}}{\omega'^2-\omega^2}d\omega' \qquad \text{(III.3)}$$

P : is the principal value of the integral given as.

$$P = \lim_{a\to 0}\int_{-\infty}^{\omega-a}\frac{\varepsilon(\omega')}{\omega'-\omega}d\omega' + \lim_{a\to 0}\int_{\omega-a}^{+\infty}\frac{\varepsilon(\omega')}{\omega'-\omega}d\omega' \qquad \text{(III.4)}$$

Penn's model [12] expresses the link between the static dielectric constant $\varepsilon_1(0)$ of a semiconductor compound and its fundamental energy gap E_g and the plasma energy $\hbar\omega$ by :

$\varepsilon_1(0)=1+(\hbar\omega/E_g)$.

The real and imaginary parts of complex dielectric function $\varepsilon(\omega)$ for semiconductor compound $CuGaO_2$ are shown in ***figure*(*III*.6)**, which have been calculated under

condition of illumination light less than or equal to 30 eV. The static dielectric constant ε_1 (0) obtained at zero pressure was about 4.51.

The observed peaks are mainly produced from the electronic transition of the valence band to the states forming the conduction band's orbitals .

Also , we are not interested in indirect transition that is introducing phonons vibration and weakly contributing in $\varepsilon(\omega)$. Furthermore, the beginning of the energetic spectrum $\varepsilon_2(\omega)$ is corresponding to a transition close to the direct fundamental gap (G-G) 1,489 eV.

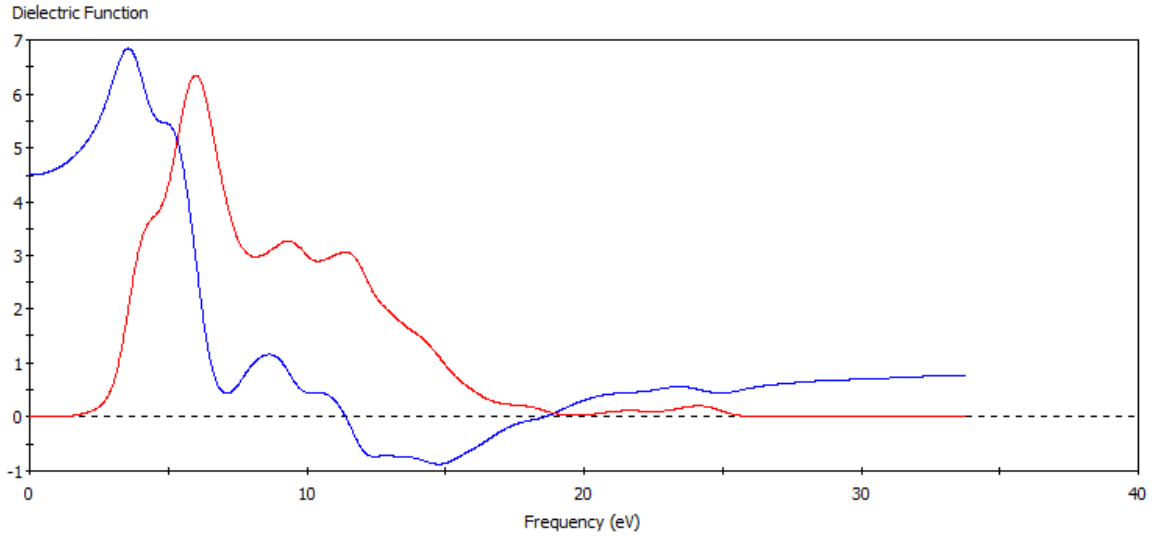

***Figure*(*III*.6):** Dielectric function, the real part $\varepsilon_1(\omega)$ (in bleu) and the imaginary part $\varepsilon_2(\omega)$ (in red), of **$CuGaO_2$**.

III. 4.2. Optical absorption :

Optical absorption coefficient is given as function of the real and imaginary parts of the dielectric function by the following expression:

$$I(\omega) = \sqrt{2}(\omega)\left(\sqrt{\varepsilon_1(\omega)^2 + \varepsilon_2(\omega)^2} - \varepsilon_1(\omega)\right)^{1/2} \qquad \text{(III.5)}$$

The linear optical absorption spectrum $I(\omega)$ are depicted in ***figure*(*III*.7).**

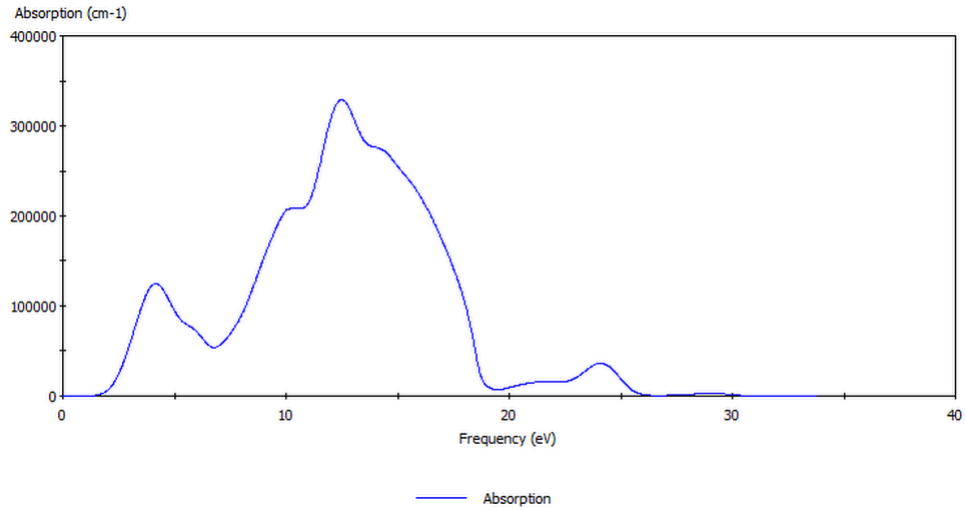

***Figure*(*III*.7):** Linear absorption spectrum *I(ω)*of **$CuGaO_2$**.

For our compound the absorption start in about 0,7 eV corresponds the gap H_v-G_c (0,718 eV) which corresponds to the electronic transition between the valence band and the conduction band. This is known as fundamental absorption threshold, which originates from transitions of O 2p and Cu 3d electrons of the valence band to the Ga 3s empty orbitals dominating the deep conduction band..

III. 4.3. Refractive index:

The refractive index is one of the most important optical constants. Generally, it depends on the wavelength of the electromagnetic wave. The case where an electromagnetic wave can lose its energy during the propagation, the refractive index becomes complex; A real part is usually the refractive index *n* and the imaginary part is called the extinction coefficient *k*. They can be expressed as:

$$n(\omega) = \left[\frac{\varepsilon_1(\omega)}{2} + \frac{\sqrt{\varepsilon_1(\omega)^2+\varepsilon_2(\omega)^2}}{2}\right]^{1/2} \quad \text{(III.6)}$$

$$k(\omega) = \left[\frac{\sqrt{\varepsilon_1(\omega)^2+\varepsilon_2(\omega)^2}}{2} - \frac{\varepsilon_1(\omega)}{2}\right]^{1/2} \quad \text{(III.7)}$$

The refractive indices *n* (ω) and extinction index *K* (ω) spectrum of our compound, are illustrated in ***figure*(*III*.8)**. At zero pressure, the static refractive index *n* (0) is found to be 2.52. Moreover, the refractive index spectrum increases with the photon energy evolution in the visible range of the solar spectrum and then a peak in the ultraviolet region at about 12.3 eV**.**

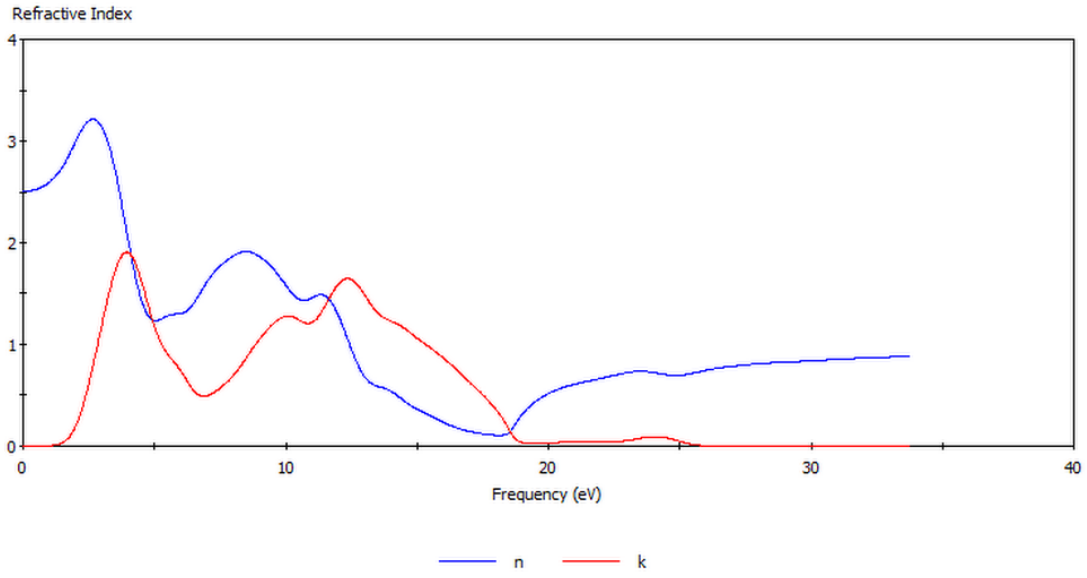

***Figure*(*III*.8):** The refractive index *n*(ω)(in bleu) and the extinction *k*(ω) (in red) spectrums of **$CuGaO_2$.**

III. 4.4.Reflectivity and optical loss :

The reflectivity *R(ω)* and the optical loss *L(ω)* are given by the two following expressions [13. 14]:

$$R(\omega) = \left|\frac{\varepsilon^{1/2}(\omega)-1}{\varepsilon^{1/2}(\omega)+1}\right|^2 \qquad \text{(III.8)}$$

$$L(\omega) = -Im\left(\frac{1}{\varepsilon(\omega)}\right) = \frac{\varepsilon_2(\omega)}{\varepsilon_1^2(\omega)+\varepsilon_2^2(\omega)} \qquad \text{(III.9)}$$

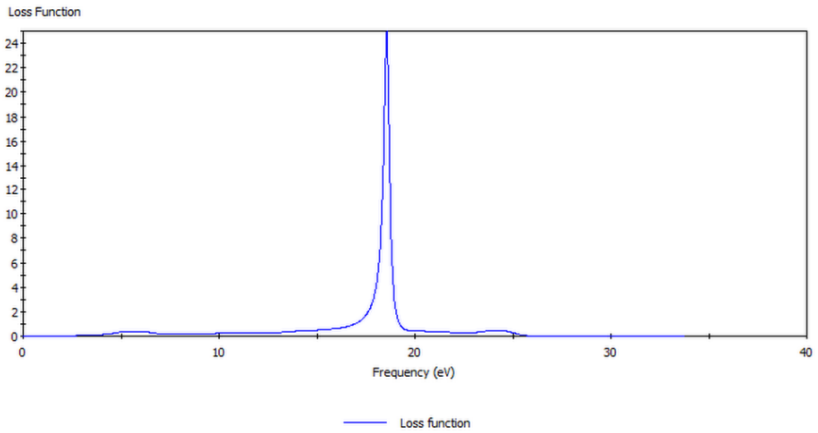

***Figure*(*III*.9)** shows the reflectivity *R* (ω) and loss function *L* (ω) spectrum. From this figure it is clear that the most pronounced peak of *L* (ω) is located at 18,6 eV. This corresponds to the beginning of the abrupt decrease of the intensity of *R* (ω). This result can be used as a theoretical basis for the experimenters and for the $CuGaO_2$'s potential application into optical devices design field such as protection shield against the UV radiation or into a solar cell.

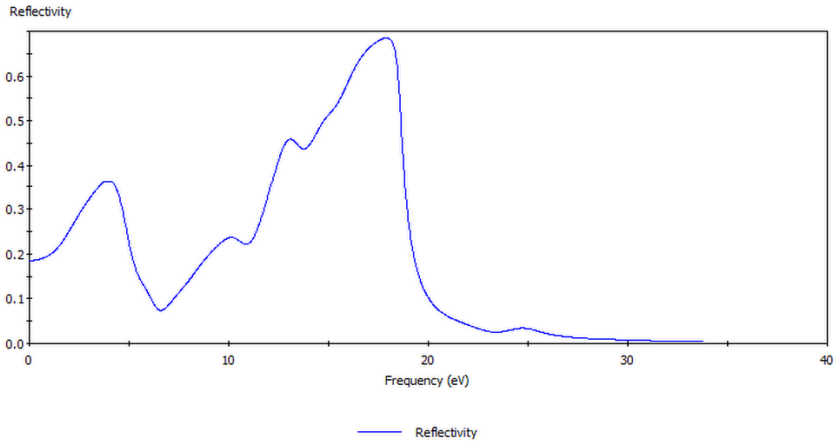

***Figure*(*III*.9):** Reflectivity *R(ω)* and loss function *L(ω)* of $CuGaO_2$.

III. 4.5. Elastic properties :

The elastic properties of solids are of great interest for knowing important information about the mechanics and dynamic properties of materials, the nature of the forces operated on solids and structural stability. They are determined from linear adjustment of stresses-strain according to Hook's law after geometry optimization of the structure.

III. 4.5.1. Elastic constants for monocrystalline state :

The hexagonal system has five independent elastic constants C_{11},C_{12}, C_{13}, C_{33} and C_{44}. C_{66} Can be estimated from C_{11} and C_{12} using the relation :$C_{66} = (C_{11} - C_{12})/2$.

For our compound $CuGaO_2$ we calculated anisotropic values of elastic constants C_{ij}(in GPa), Young's modulus *E*, bulk modulus *B*, Poisson's ratio under zero pressure condition. The calculated results are listed in (***III*.4**) **.**

The material studied is characterized by a high values of C_{11} and C_{33} compared to others ones. This does mean that it is more resistant to unidirectional compression than to shear deformations. In addition, the high value of the elastic constant C_{33} reflects the hardness of the Cu-O covalent bond which lies along the main direction [0001].
Generally, our values of the elastic constants are close to those reported in the reference [5].

***Table*(*III*.4):** Elastic constants C_{ij}, Young's modulus E_X,E_Y, E_Z, bulk modulus *B*, Poisson's ratio E_{XY}, E_{YX}, E_{ZX},E_{XZ}, E_{YZ} and E_{ZY} calculated under 0 GPa.

Parameter	**This work**	**Other calculation [5]**
C_{11} C_{12}	217.93 76.87	217.7, 76.9
C_{13}	94.33	95.2
C_{33} C_{44}	450.52262 38.87752	452.5 45.3
B (GPa)	140.52	149.4

Ex	181.71586	
Ey	181.71586	
Ez	390.15485	
Exy Exz (GPa)	0.2882 0.1490	
Eyx Eyz(GPa)	0.2882 0.1490	
Ezx Ezy (GPa)	0.3200 0.3200	

III. 4.5.2. Mechanical stability :

The mechanical stability of a hexagonal system requires from the five independent elastic constantC_{11}, C_{12}, C_{13}, C_{33} and C_{44} to obey the following Born's condition [15-16]:

$$\begin{cases} C_{11} > |C_{12}|; & 2\,C_{13}^{\,2} < C_{33}(C_{11} + C_{12}) \\ C_{44} > 0;\ C_{66} > 0 \end{cases} \qquad (III.10)$$

III. 4.5.3. Elastic properties for polycrystalline state :

The only way to establish polycrystalline elasticity modulus from ab-initio calculations is to firstly, calculate the monocrystalline elastic constants then transform them to a macroscopic quantities using methods allowing to calculate the average values based on the static mechanics. The values of these isotropic modulus are based on the most frequently used methods that we discussed in the previous chapter (Voigt, Reuss and Hill).

Isotropic elastic modulus , compressibility's modulus *B*, Lamé coefficient λ et μ (shear module) under P=0 GPa, are gathered in the table below.

***table*(*III*.4):** Isotropic elastic modulus calculated under 0 P=GPa.

Parameter	Voigt	Reuss	Hill
B	157.49368	140.51825	149.00596
$\boldsymbol{\lambda}$	110.12898	102.64644	106.38771
$\boldsymbol{\mu}$	71.04705	56.80771	63.92738

Additionally, the ductility of a material can be roughly estimated by the value of bulk modulus to shear modulus ratio (B/G) ; empirical formula proposed by Pugh [17], For $B/G > 1.75$, the material is ductile, otherwise, for B/G 1.75, the material is intractable. The B / G ratio value is greater than 1.75 for our compound. Therefore it should be classified as ductile material.

Bibliographies:

[1] S. J. Clark, M. D. Segall, C. J. Pickard, P. J. Hasnip, M. J. Probert, K. Refson, M. C. Payne. Z. Kristallogr. 220 (2005) 567–570.

[2] V. Jayalakshmi, R. Murugan, B. Palanivel, J. Alloys Compd. 388 (2005) 19.

[3] A. Buljan, P. Alemany, E. Ruiz, J. Phys. Chem. B 103 (1999) 8060.

[4] H.C. Kandpal, R. Seshadri, Solid State Sci. 4 (2002) 1045.

[5] Q.J. Liu, Z.T. Liu, J.C. Chen, L.P. Feng, H.Tian. Physica B 406 (2011) 3377.

[6] A. Buljan, P. Alemany, E. Ruiz, J. Phys. Chem. B 103 (1999) 8060.

[7] H. Yanagi, H. Kawazoe, A. Kudo, M. Yasukawa, H. Hosono, J. Electroceram. 4 (2000) 407.

[8] K. Ueda, T. Hase, H. Yanagi, H. Kawazoe, H. Hosono, H. Ohta, M. Orita, M. Hirano, J. Appl. Phys. 89 (2001) 1790.

[9] R. Besma, Etude des propriétés structurales, électroniques, optiques et élastiques du composé 3R-CuGaO2. Mémoire de Master, Université M^{ed} Boudiaf, M'sila-Algérie. 2016.

[10] Kh. HADDADI, Etude des propriétés structurales, élastiques et électroniques des composés antiperovskites de type XNCa3, Thèse de doctorat, Université Ferhat Abbas de Sétif, Algérie. 2013.

[11] M.A. Khan, A. Kasphyop, A. K. Solanki, T. Nautiyal, and S. auluck, Phys. Rev. B 23 (1993) 16974.

[12] D.R. Penn, Phys. Rev 128 (1962) 2093.

[13] Y. Zhang, W.M. Shen, Basic of Solid Electronics, Zhe Jiang University Press, Hangzhou, 2005.

[14] C.M.I. Okoye, J. Phys.: Condens. Matter 15 (2003) 5945.

[15] M. Born, Proc. Cambridge Philos. Soc., 36 (1940) 160.

[16] M. Born et K. Huang, Dynamical Theory of Crystal Lattices, édité par Clarendon, Oxford (1956).

[17] S.F. Pugh, Phil. Mag. 45 (1954) 823.

GENERAL CONCLUSION

General conclusion

The structural, electronic (electronic band structure, density of states Mulliken's population analysis, charge density of valence electrons**)**,optical (dielectric function, optical absorption, refractive index, reflectivity and optical loss) and elastic properties (elastic constants for monocrystalline and polycrystalline states and mechanical stability) of the 2H-CuGaO2 compound have been studied in this work, by using the plane-wave ultrasoft pseudo-potential methods and the generalized gradient approximation (GGA) to describe the exchange-correlation energy within the density-functional theory as implemented in the CASTEP code.

First, we studied the structural properties in order to characterize the fundamental state of the considered system. However, our values show little overestimation compared with the experimental ones ; It is well known that in general the GGA overestimates the structural parameters, whereas the LDA underestimates them.

Second, the electronic properties such as density of states, charge density and band structures have been presented. The 2H-CuGaO2 compound shows an indirect band gap (**G-H**); the valence band maximum (VBM) is located at **H** point and the conduction band minimum (CBM) is located at **G** point. Furthermore, our values of energy band gap are closer to theoretical values, which are also calculated in the frame work of the DFT. The deviations of our results of the indirect and direct band gap from the theoretical ones are acceptable.

In addition, we calculated the density of charges into the plan $(11\bar{2}0)$ in order to take a general idea about the nature of chemical bonding in the crystalline solid CuGaO2 and to understand briefly the bonds mechanism linking the cations and the anions. The large transfer of charges from the cation to the anion indicates that the anion has a higher electronegativity than that of the cation. Furthermore, the high ionic valence of Cu

compared to Ga indicates that the Cu-O bond is much more covalent than the Ga-O bond. This latter has coexistence between the ionic and covalent bonds.

The optical properties such as dielectric function and absorption coefficient, refractive and reflectivity index have been also calculated in order to study the behavior of the semiconductor $CuGaO_2$ versus incident light. We found that the absorption starts in about 0,7 eV which corresponds to the electronic transition between the valence band and the conduction band (indirect band gap H-G : 0,718 eV). This is known as fundamental absorption threshold, which originates from transitions of O 2p and Cu 3d electrons of the valence band to the Ga 3s empty orbitals dominating the deep conduction band. Also, the refractive index spectrum increases with the photon energy evolution in the visible range of the solar spectrum and then a pronounced peak is observed in the ultraviolet region. Furthermore, the most pronounced peak of L (ω) is located at 18,6 eV. This corresponds to the beginning of the abrupt decrease of the intensity of R (ω). This result can be used as a theoretical basis for the experimenters and for the CuGaO2's potential application in optical devices design field such as protection shield against the UV radiation or in a solar cell.

On the other hand, we calculated the elastic properties of the 2H-CuGaO2 compound such as anisotropic values of elastic constants ,Young's modulus *E*, bulk modulus *B*, Poisson's ratio to get important information about the mechanics and dynamic properties of the compound. Our results of elastic constants are somewhat higher compared to others ones. This is due to the different initial parameters used in each calculation. Also, the obtained elastic constants C_{ij} demonstrated the mechanical stability of the hexagonal structure of 2H-CuGaO2.

Finally, it is worth noting that the CASTEP code is a very powerful tool which allows easy and direct calculation of the different properties of the matter despite of our modest and short experience of using it.

List of Figures

List of Tables

ملخص

الخصائص البنيوية، الإلكترونية (مستويات الطاقة الإلكترونية . خصائص الروابط الكيميائية، كثافة الحالات الإلكترونية الجزئية و الكلية (TDOS- PDOS) و مخططات التوازيع الإلكترونية التكافئية)، المرونية(ثابت مرونة، معامل المرونة والاستقرار الميكانيكي) و الضوئية (معامل العزل ، معامل الامتصاص، و انعكاسية، معامل الانكسار) للمركب (2H–CuGaO2) تم حسابها في هذا البحث في إطار نظرية دالية الكثافة الإلكترونية(DFT) إضافة إلى نظرية الكمونات الكاذبة (PPs) و الأمواج المستوية (PWs). باستعمال تقريب التدرج المعمم (GGA) لطاقة التبادل–الارتباط ببرنامج"CASTEP". وقد تم تحسين هندسة المركب المدروس (2H-CuGaO2) في حالة التوازن لضغط معدوم. نتائجنا تم مقارنتها مع النتائج التجريبية والنظرية المتاحة.

الكلمات المفتاحية :DFT, CASTEP code , **الكمون** الكاذب (PP)،**الامواج المستوية**(PW)، **2H**-CuGaO2.

Abstract

The structural, electronic (electronic band structure, properties of chemical bonds, density diagrams of total and partial electronic states (TDOS and PDOS) and the valence electronic charge distribution maps), elastic (elastic constants, bulk modulus, shear modulus, Young's modulus, Poisson rates and mechanical stability) and optical (dielectric function, absorption coefficient, reflectivity, refractive index) properties of 2H-CuGaO2 compound were calculated in this work within the formalism of density functional theory (DFT) with pseudopotentials (PPs), plane waves (PWs) approach and the generalized gradient approximation (GGA) for energy exchange-correlation using CASTEP code. The equilibrium geometry of the studied compound (2H-CuGaO2) has been optimized at zero pressure. Our results were compared with available experimental and theoretical ones.

Key words: DFT, CASTEP code, Pseudopotential (PP), Plane wave (PW), 2H-CuGaO2.

Résumé

Les propriétés structurales, électroniques (structure de bandes électroniques, propriétés des liaisons chimiques, les diagrammes de densité d'états électroniques totale et partielle (TDOS et PDOS) et les cartes de distribution de charges électroniques de valence), élastiques (constantes élastiques, module de compressibilité, module de cisaillement, module de Young, rapport de Poisson et stabilité mécanique) et optiques (fonction diélectrique, coefficient d'absorption, réflectivité, indice de réfraction) du composé 2H-$CuGaO_2$ ont été calculées dans ce travail dans le cadre du formalisme de la théorie de la fonctionnelle de la densité (DFT) avec l'approche des pseudopotentiels (PPs), les ondes planes (PWs) et l'approximation du gradient généralisé (GGA) pour l'énergie d'échange-corrélation en utilisant le code CASTEP. La géométrie d'équilibre du composé étudié (2H-$CuGaO_2$) a été optimisée à pression nulle. Notre résultats sont comparés avec les résultats expérimentaux et théoriques disponibles.

Mots clés : DFT, CASTEP code, Pseudopotential (PP), Plane wave (PW), 2H-CuGaO2.